Angewandte Chemie
Eine Zeitschrift der Gesellschaft Deutscher Chemiker

Supporting Information

An NIR Fluorescence Turn-on and MRI Bimodal Probe for Concurrent Real-time in vivo Sensing and Labeling of β-Galactosidase

*Q. Yu, L. Zhang, M. Jiang, L. Xiao, Y. Xiang, R. Wang, Z. Liu, R. Zhou, M. Yang, C. Li, M. Liu, X. Zhou, S. Chen**

SUPPORTING INFORMATION

Table of Contents

SUPPORTING INFORMATION

1. Experimental Section

1.1. Materials

4-hydroxybenzaldehyde, 2-(acetoxymethyl)-6-bromotetrahydro-2H-pyran-3,4,5-triyl triacetate, 2,4-dihydroxybenzaldehyde, 1,4,7,10-tetraazacyclododecane, 2,3,3-Trimethylindolenine, Tetrabutylammonium bromide, and Benzyl N-(2-aminoethyl)carbamate hydrochloride, 5-Chloro-1-pentyne, tert-Butyldimethylsilyl chloride, Imidazole, O-(7-Azabenzotriazol-1-yl)-N,N, N',N'-tetramethyl uranium hexafluorophosphate, Gadolinium(III) chloride hexahydrate and (E)-2-chloro-3-(hydroxymethylene)cyclohex-1-ene-1-carbaldehyde were purchased from Shanghai Bede Pharmaceutical Co., Ltd; Phosphorus tribromide, t-butyl 2-bromoacetate, Sodium borohydride, 2-azidoacetic acid, isocyanatoethane, resorcinol, N,N-Diisopropylethylamine, 10% Pd/C and 2-bromoacetyl bromide were purchased from Discovery Technology Co., Ltd; Concentrated hydrochloric acid, Sodium hydroxide, Potassium carbonate, Sodium acetate, Potassium bicarbonate, Potassium iodide, Sodium hydride, Sodium methoxide, Cupric sulfate, Sodium ascorbate and other solvents were purchased from Chinese Pharmaceutical Co., Ltd; *β*-Galactosidases from Escherichia coli was purchased from Beijing Solarbio Science & Technology Co., Ltd and BSA (bovine serum albumin) from Aladdin; The 200-300 mesh TLC silica-gel powder was purchased from Qingdao Foreign Chemical Industry Co., Ltd; SKOV3 cells and 293T cells were obtained from Cell Bank of the Chinese Academy of Sciences (Shanghai, China). BALB/c nude mice were purchased from Wuhan Bainte Biotechnology Co., Ltd; Pure water /ultra-pure water was prepared and purified by a Milli-Q reference system (Millipore).

1.2. Instrumentation

The ^{1}H and ^{13}C NMR spectra were acquired on a 500 MHz Bruker spectrometer. High-performance liquid chromatography (HPLC) was carried out on Shimadzu LC-20A with CH_3CN/H_2O (1‰ CF_3COOH) as the eluents. High-resolution mass spectra (HRMS) were recorded on a Bruker micro-TOF-QII time-of-flight mass spectrometer with electrospray ionization. The UV-vis spectra were carried out on an EVOLUTION-220 UV−vis spectrometer (Thermo Scientific, USA). The fluorescence spectra were measured with an Edinburgh FS5 fluorescence spectrometer with a 150 W xenon lamp. Fluorescence scanning in the gel was taken using Gel Doc^{TM} XR+Gel Documentation System with Image Lab Software (Bio-Rad, USA). MR relaxivities were acquired on a 0.5 T MR scanner (Bruker, Germany) *in vitro* and *in vivo* MR imaging experiments were performed on a 9.4 T MR scanner (Bruker, Germany). Fluorescent images of cells were acquired with a fluorescence microscope (Nikon, Japan). MTT assay was performed on a microplate reader (Spectra Max 190). Whole-body fluorescence images were acquired with IVIS Lumina XRMS Series III *in vivo* Imaging System (PerkinElmer, Inc. USA).

2. Chemical Synthesis of Compounds

2.1. Synthesis of Gal-Cy-Gd-1

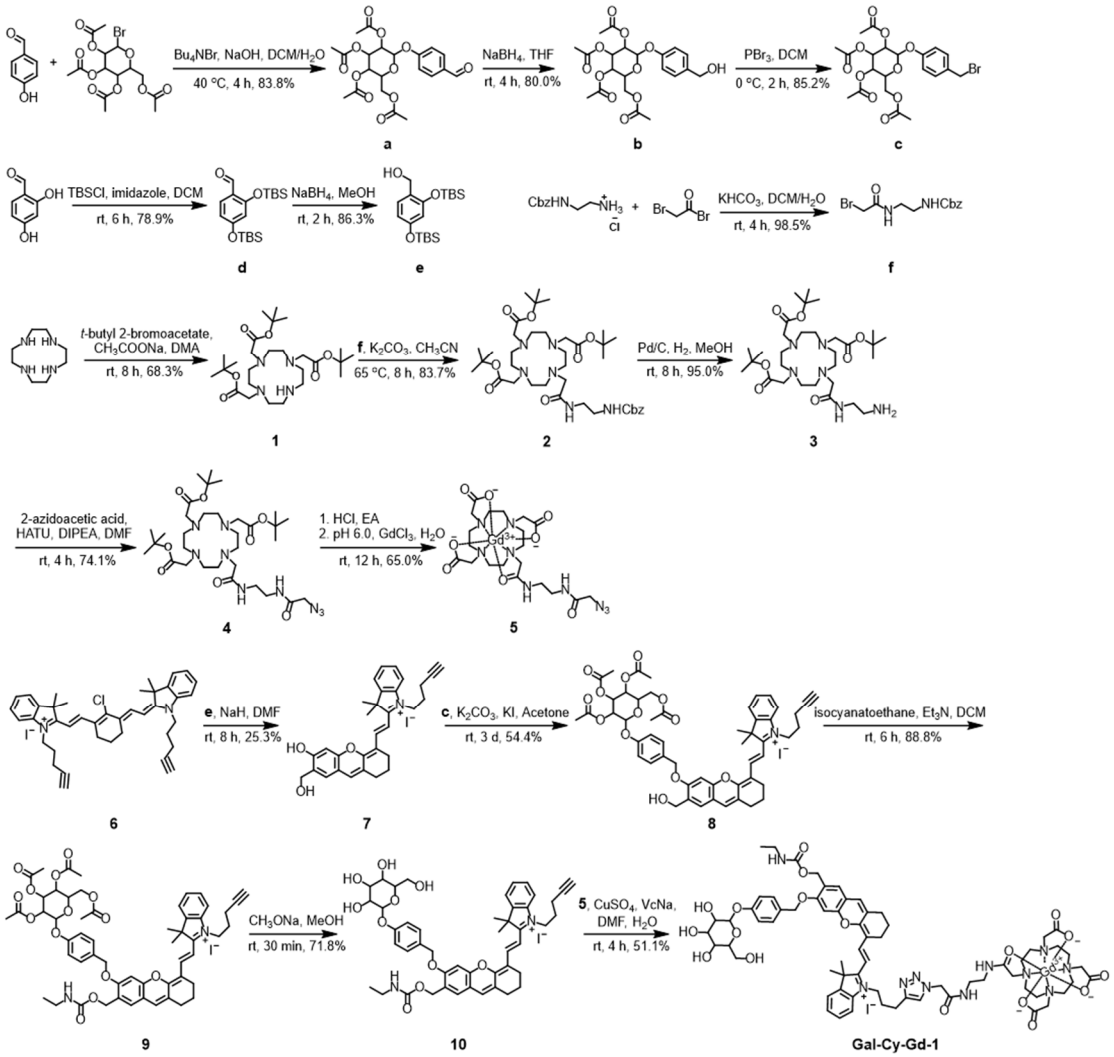

Scheme S1. Synthetic routes of Gal-Cy-Gd-1.

2-(acetamidomethyl)-6-(4-formylphenoxy)tetrahydro-2H-pyran-3,4,5-triyl triacetate (a)

To a solution of 4-hydroxybenzaldehyde (2.0 g, 16.4 mmol), 2-(acetoxymethyl)-6-bromotetrahydro-2H-pyran-3,4,5-triyl triacetate (13.5 g, 32.7 mmol) and Bu_4NBr (5.3 g, 16.4 mmol) in CH_2Cl_2 (200 mL), a solution of 5% NaOH (1.83 g, 45.7 mmol) in H_2O (36.6 mL) was added, and the reaction was stirred at ambient temperature for 4 h. Then the solution was transferred to the separation funnel, and the aqueous layer was extracted with CH_2Cl_2 (3 × 100 mL). The combined organic layers were dried over anhydrous Na_2SO_4 and concentrated. The residue was purified by chromatography on silica gel column (petroleum ether/ethyl acetate = 2:1) to afford the product **a** (6.2 g, 83.8%) as a white solid. ^1H NMR (500 MHz, $CDCl_3$): δ 9.86 (s, 1H), 7.80 – 7.79 (d, *J* = 8.7 Hz, 2H), 7.07 – 7.06 (d, *J* = 8.7 Hz, 2H), 5.46 – 5.45 (m, 1H), 5.42 (d, *J* = 3.0 Hz, 1H), 5.17 – 5.16 (d, *J* = 8.0 Hz, 1H), 5.11 – 5.10 (dd, *J* = 10.5, 3.3 Hz, 1H), 4.18 – 4.15 (m, *J* = 13.3, 9.3 Hz, 1H), 4.13 – 4.10 (m, *J* = 13.2, 5.8 Hz, 2H), 2.12 (s, 3H), 2.00 (d, *J* = 4.4 Hz, 6H), 1.95 (s, 3H). HRMS (ESI) Calcd for $[C_{21}H_{24}O_{11}, M + Na]^+$: 475.1216, Found: 475.1385.

2-(acetoxymethyl)-6-(4-(hydroxymethyl)phenoxy)tetrahydro-2H-pyran-3,4,5-triyl triacetate (b)

To a solution of the compound **a** (3.0 g, 6.6 mmol) in THF (150 mL), sodium borohydride (250.8 mg, 6.6 mmol) was added carefully in portions at 0 °C. After being stirred at ambient temperature for 4 h, THF was evaporated *in vacuo*. A combined solution of saturated NH_4Cl (200 mL) and CH_2Cl_2 (250 mL) was added, the two phases were separated, and the aqueous layer was extracted with CH_2Cl_2 (3 × 50 mL). The combined organic layers were dried over anhydrous Na_2SO_4 and concentrated. The residue was purified by chromatography on silica gel column (petroleum ether/ethyl acetate = 1:1) to afford the product **b** (2.4 g, 80.0%) as a white solid. ^{1}H NMR (500 MHz, $CDCl_3$): δ 7.31 – 7.30 (d, *J* = 8.6 Hz, 2H), 7.01 – 6.99 (d, *J* = 8.6 Hz, 2H), 5.49 – 5.45 (m, 2H), 5.12 – 5.10 (dd, *J* = 10.5, 3.4 Hz, 1H), 5.04 – 5.02 (d, *J* = 8.0 Hz, 1H), 4.65 (s, 2H), 4.25 – 4.21 (m, *J* = 11.3, 7.0 Hz, 1H), 4.18 – 4.10 (m, 2H), 4.07 – 4.05 (t, *J* = 6.7 Hz, 1H), 2.19 (s, 3H), 2.07 – 2.06 (d, *J* = 2.6 Hz, 6H), 2.02 (s, 3H). HRMS (ESI) Calcd for $[C_{21}H_{26}O_{11}$, M + Na$]^+$: 477.1373, Found: 477.1545.

2-(acetoxymethyl)-6-(4-(bromomethyl)phenoxy)tetrahydro-2H-pyran-3,4,5-triyl triacetate (c)

To a solution of compound **b** (2.4 g, 5.3 mmol) in CH_2Cl_2 (200 mL), PBr_3 (714.9 mg, 2.6 mmol) was added carefully at 0 °C, and the reaction was stirred at ambient temperature for 2 h. The solution of saturated $NaHCO_3$ (20 mL) was added dropwise before further dilution with water (200 mL), the two phases were separated, and the aqueous layer was extracted with CH_2Cl_2 (3 × 50 mL). The combined organic layers were dried over anhydrous Na_2SO_4 and concentrated. The residue was purified by chromatography on silica gel column (petroleum ether/ethyl acetate = 5:1) to afford the product **c** (2.3 g, 85.2%) as a white solid. ^{1}H NMR (500 MHz, $CDCl_3$): δ 7.30 – 7.29 (d, *J* = 8.6 Hz, 2H), 6.94 – 6.93 (d, *J* = 8.6 Hz, 2H), 5.46 – 5.42 (m, 2H), 5.10 – 5.07 (dd, *J* = 10.4, 3.4 Hz, 1H), 5.04 – 5.03 (d, *J* = 7.9 Hz, 1H), 4.44 (s, 2H), 4.20 – 4.11 (m, *J* = 17.4, 11.3, 6.6 Hz, 2H), 4.07 – 4.04 (t, *J* = 6.7 Hz, 1H), 2.14 (s, 3H), 2.03 – 2.02 (d, *J* = 2.0 Hz, 6H), 1.98 (s, 3H). HRMS (ESI) Calcd for $[C_{21}H_{25}BrO_{10}$, M + COOH$]^-$: 561.0613, Found: 561.0807.

2,4-bis((tert-butyldimethylsilyl)oxy)benzaldehyde (d)

To a solution of 2,4-dihydroxybenzaldehyde (5.0 g, 36.2 mmol) and imidazole (14.8 g, 217.2 mmol) in CH_2Cl_2 (400 mL), a solution of tert-butyldimethylsilyl chloride (16.4 g, 108.6 mmol) in CH_2Cl_2 (150 mL) was added dropwise, and the reaction was stirred at ambient temperature for 6 h. Saturated NH_4Cl (350 mL) was added, the two phases were separated, and the aqueous layer was extracted with CH_2Cl_2 (3 × 100 mL). The combined organic layers were dried over anhydrous Na_2SO_4 and concentrated. The residue was purified by chromatography on silica gel column (petroleum ether/ethyl acetate = 50:1) to afford the product **d** (10.5 g, 78.9%) as a pale yellow oil. ^{1}H NMR (500 MHz, $CDCl_3$): δ 10.29 (s, 1H), 7.72 – 7.71 (d, *J* = 8.6 Hz, 1H), 6.51 – 6.50 (dd, *J* = 8.6, 1.3 Hz, 1H), 6.29 (d, *J* = 2.0 Hz, 1H), 1.01 – 0.97 (d, *J* = 30.4 Hz, 18H), 0.27 – 0.23 (d, *J* = 32.1 z, 12H). HRMS (ESI) Calcd for $[C_{19}H_{34}O_3Si_2$, M + H$]^+$: 366.2046, Found: 367.2307.

(2,4-bis((tert-butyldimethylsilyl)oxy)phenyl)methanol (e)

To a solution of the compound **d** (16.0 g, 43.6 mmol) in MeOH (300 mL), sodium borohydride (1.65 g, 43.6 mmol) was added carefully in portions at 0 °C. After being stirred at ambient temperature for 2 h, methanol was evaporated *in vacuo*. A combined solution of saturated NH_4Cl (300 mL) and CH_2Cl_2 (150 mL) was added, the two phases were separated, and the aqueous layer was extracted with CH_2Cl_2 (3 × 100 mL). The combined organic layers were dried over anhydrous Na_2SO_4 and concentrated. The residue was purified by chromatography on silica gel column (petroleum ether/ethyl acetate = 20:1) to afford the product **e** (10.5 g, 78.9%) as a pale yellow oil. ^{1}H NMR (500 MHz, $CDCl_3$): δ 7.13 – 7.11 (d, *J* = 8.2 Hz, 1H), 6.45 – 6.43 (dd, *J* =

8.2, 2.3 Hz, 1H), 6.33 (d, *J* = 2.3 Hz, 1H), 4.59 (s, 2H), 1.02 (s, 9H), 0.98 (s, 9H), 0.26 (s, 6H), 0.19 (s, 6H). HRMS (ESI) Calcd for $[C_{19}H_{36}O_3Si_2, M + Na]^+$: 391.2101, Found: 391.2262.

benzyl (2-(2-bromoacetamido)ethyl)carbamate (f)

To a mixture of 2-(((benzyloxy)carbonyl)amino)ethan-1-aminium chloride (5.0 g, 21.7 mmol) in CH_2Cl_2 (200 mL), $KHCO_3$ (10.8 g, 108.5 mmol) in H_2O (50 mL), a solution of 2-bromoacetyl bromide (5.2 g, 26.0 mmol) in CH_2Cl_2 (100 mL) was added dropwise at 0 °C, and the reaction was stirred at ambient temperature for 4 h. Then the solution was transferred to the separation funnel, and the aqueous layer was extracted with CH_2Cl_2 (3 × 100 mL). The combined organic layers were dried over anhydrous Na_2SO_4 and concentrated to afford the product **f** (6.7 g, 98.5%) as a white solid. ^{1}H NMR (500 MHz, $CDCl_3$): δ 7.38 – 7.32 (m, 5H), 5.10 (s, 2H), 3.81 (s, 2H), 3.42 – 3.35 (m, 4H).

tri-tert-butyl 2,2',2''-(1,4,7,10-tetraazacyclododecane-1,4,7-triyl)triacetate (1)

To a mixture of 1,4,7,10-tetraazacyclododecane (2.0 g, 11.6 mmol) and CH_3COONa (2.8 g, 34.8 mmol) in DMA (100 mL), a solution of t-butyl 2-bromoacetate (6.8 g, 34.8 mmol) in DMA (100 mL) was added dropwise at 0 °C, and the reaction was stirred at ambient temperature for 8 h. Then the mixture was filtered and solid part was washed three times with DMA (10 mL). The filtrates were combine and concentrated to afford the product **1** as a white solid. ^{1}H NMR (500 MHz, $CDCl_3$): δ 3.33 (s, 4H), 3.24 (s, 2H), 3.05 (s, 4H), 2.88 – 2.82 (d, *J* = 27.8 Hz, 12H), 1.41 – 1.40 (d, *J* = 2.8 Hz, 27H). HRMS (ESI) Calcd for $[C_{26}H_{50}N_4O_6, M + H]^+$: 515.3809, Found: 515.4320.

tri-tert-butyl 2,2',2''-(10-(2-((2-(((benzyloxy)carbonyl)amino)ethyl)amino)-2-oxoethyl)-1,4,7,10-tetraazacyclododecane-1,4,7-triyl)triacetate (2)

To a solution of the compound **1** (3.0 g, 5.8 mmol) and K_2CO_3 (1.9 g, 13.9 mmol) in CH_3CN (150 mL), a solution of the compound **f** (2.2 g, 7.0 mmol) in CH_3CN (100 mL) was added, and the reaction was stirred for 8 h at 65 °C. Then the mixture was filtered and the solid part was washed three times with CH_3CN (20 mL). The filtrates were combined and concentrated. The residue was purified by chromatography on silica gel column (CH_2Cl_2/MeOH = 100:3) to afford product **2** (3.6 g, 83.7%) as a white solid. ^{1}H NMR (500 MHz, $CDCl_3$): δ 7.31 – 7.30 (d, *J* = 7.3 Hz, 2H), 7.27 – 7.24 (m, 2H), 7.21 – 7.18 (t, *J* = 7.2 Hz, 1H), 5.02 (s, 2H), 3.33 (s, 9H), 2.95 – 2.03 (m, 19H), 1.40 – 1.37 (d, *J* = 12.3 Hz, 27H). HRMS (ESI) Calcd for $[C_{38}H_{64}N_6O_9, M + Na]^+$: 771.4632, Found: 771.5256.

tri-tert-butyl 2,2',2''-(10-(2-((2-aminoethyl)amino)-2-oxoethyl)-1,4,7,10-tetraazacyclododecane-1,4,7-triyl)triacetate (3)

Compound **2** (1.0 g, 1.3 mmol) was stirred over Pd/C (100 mg, 10 % by wt.) in MeOH under 1 atm H_2(g). After 8 h, the mixture was filtered to remove Pd/C and the solid part was washed three times with CH_2Cl_2 (10 mL). The filtrates were combined and concentrated to afford product **3** as a white solid. ^{1}H NMR (500 MHz, $CDCl_3$): δ 3.62 (s, 2H), 3.47 – 3.18 (m, 8H), 2.81 – 2.22 (m, 18H), 1.45 (s, 27H). HRMS (ESI) Calcd for $[C_{30}H_{58}N_6O_7, M + Na]^+$: 637.4265, Found: 637.4480.

tri-tert-butyl 2,2',2''-(10-(2-((2-(2-azidoacetamido)ethyl)amino)-2-oxoethyl)-1,4,7,10-tetraazacyclododecane-1,4,7-triyl)triacetate (4)

To a mixture of 2-azidoacetic acid (473.4 mg, 4.7 mmol) and HATU (1.5 g, 3.9 mmol) in DMF (50 mL), a solution of DIPEA (756.1 mg, 5.9 mmol) and the compound **3** (2.4 g, 3.9 mmol) in DMF (50 mL) was added, and the

reaction was stirred at ambient temperature for 4 h. Then the mixture was concentrated and extracted with CH_2Cl_2 (200 mL) and H_2O (200 mL). The organic layer was dried over anhydrous Na_2SO_4 and concentrated. The residue was purified by chromatography on silica gel column (CH_2Cl_2/MeOH = 100:3) to afford the product **4** (6.7 g, 98.5%) as a white solid. ^{1}H NMR (500 MHz, $CDCl_3$): δ 3.89 (s, 2H), 3.36 (s, 8H), 2.80 (s, 8H), 2.66 – 2.58 (d, *J* = 40.0 Hz, 4H), 2.23 – 2.20 (m, 6H), 1.66 (s, 2H), 1.46-1.45 (d, *J* = 6.1 Hz, 27H). HRMS (ESI) Calcd for $[C_{32}H_{59}N_9O_8$, M + Na$]^+$: 720.4384, Found: 720.4649.

(E)-2-(2-(6-hydroxy-7-(hydroxymethyl)-2, 3-dihydro-1H-xanthen-4-yl)vinyl)-3, 3 -dimethyl-1-(pent-4-ynyl)-3H-indolium iodide (7)

To a solution of the compound **e** (2.1 g, 5.6 mmol), NaH (224.0 mg, 5.6 mmol) in DMF (10 mL), a solution of the compound **6**[1] (2.0 g, 2.8 mmol) in DMF (10 mL) was added, and the reaction was stirred at ambient temperature for 8 h. Then the mixture was concentrated and extracted with CH_2Cl_2 (150 mL) and saturated NH_4Cl (100 mL), and the aqueous layer was extracted with CH_2Cl_2 (3 × 50 mL). The combined organic layer was dried over anhydrous Na_2SO_4 and concentrated. The residue was purified by chromatography on silica gel column (CH_2Cl_2/MeOH = 20:1) to afford the product **7** (860.0 mg, 25.3%) as a blue solid. ^{1}H NMR (500 MHz, CD_3OD): δ 8.77 – 8.74 (d, *J* = 14.6 Hz, 1H), 7.64 – 7.62 (d, *J* = 7.5 Hz, 1H), 7.55 – 7.51 (t, *J* = 10.7 Hz, 4H), 7.43 – 7.40 (m, 1H), 6.89 (s, 1H), 6.53 – 6.50 (d, *J* = 14.6 Hz, 1H), 4.69 (s, 2H), 4.43 – 4.40 (t, *J* = 7.4 Hz, 2H), 2.82 – 2.79 (m, 2H), 2.75 – 2.72 (t, *J* = 5.9 Hz, 2H), 2.55 – 2.54 (d, *J* = 2.3 Hz, 1H), 2.42 – 2.40 (dd, *J* = 6.1, 4.1 Hz, 2H), 2.11 – 2.05 (m, *J* = 13.6, 6.8 Hz, 2H), 1.96 – 1.93 (m, 2H), 1.83 (s, 6H). HRMS (ESI) Calcd for $[C_{31}H_{32}INO_3$, M-I$]^+$: 466.2382, Found: 466.2704.

(E)-2-(2-(7-(hydroxymethyl)-6-((4-((3,4,5-triacetoxy-6-(acetoxymethyl)tetrahydro-2H-pyran-2-yl)oxy)benzyl)oxy)-2,3-dihydro-1H-xanthen-4-yl)vinyl)-3,3-dimethyl-1-(pent-4-yn-1-yl)-3H-indolium iodide (8)

A solution of the compound **7** (400 mg, 0.6 mmol), **c** (409.0 mg, 0.8 mmol), KI (219.1 mg, 1.3 mmol) and K_2CO_3 (109.2 mg, 0.8 mmol) in acetone (10 mL) was vigorously stirred at ambient temperature for 3 d. The mixture was extracted with CH_2Cl_2 (150 mL) and saturated NH_4Cl (100 mL), and the aqueous layer was extracted with CH_2Cl_2 (3 × 50 mL). The combined organic layer was dried over anhydrous Na_2SO_4 and concentrated. The residue was purified by chromatography on silica gel column (CH_2Cl_2/MeOH = 100:3) to afford the product **8** (370.0 mg, 54.4%) as a blue solid. ^{1}H NMR (500 MHz, $CDCl_3$): δ 8.65 – 8.62 (d, *J* = 14.6 Hz, 1H), 7.63 (s, 1H), 7.59 – 7.57 (d, *J* = 7.3 Hz, 1H), 7.48 – 7.40 (m, 4H), 7.37 – 7.34 (m, 1H), 7.31 (s, 1H), 7.02 – 7.00 (m, 3H), 6.44 – 6.41 (d, *J* = 14.6 Hz, 1H), 5.50 – 5.45 (m, 2H), 5.24 (s, 2H), 5.13 – 5.06 (m, 2H), 4.76 (s, 2H), 4.48 – 4.45 (t, *J* = 7.4 Hz, 2H), 4.23 – 4.19 (dd, *J* = 11.1, 6.8 Hz, 1H), 4.17 – 4.13 (dd, *J* = 11.2, 6.4 Hz, 1H), 4.12 – 4.08 (m, 1H), 2.76 – 2.71 (m, 4H), 2.48 – 2.46 (m, 2H), 2.16 – 2.15 (m, 4H), 2.13 – 2.11 (m, *J* = 9.2, 4.9 Hz, 2H), 2.06 – 2.05 (d, *J* = 7.6 Hz, 6H), 2.01 (s, 3H), 1.93 – 1.90 (dd, *J* = 11.8, 6.5 Hz, 2H), 1.88 (s, 6H). HRMS (ESI) Calcd for $[C_{52}H_{56}INO_{13}$, M-I$]^+$: 902.3746, Found: 902.3810.

(E)-2-(2-(7-(((ethylcarbamoyl)oxy)methyl)-6-((4-((3,4,5-triacetoxy-6-(acetoxymethyl)tetrahydro-2H-pyran-2-yl)oxy)benzyl)oxy)-2,3-dihydro-1H-xanthen-4-yl)vinyl)-3,3-dimethyl-1-(pent-4-yn-1-yl)-3H-indolium iodide (9)

A solution of the compound **8** (920 mg, 0.9 mmol), isocyanatoethane (1.9 mg, 26.8 mmol) and triethylamine (Et_3N, 450.3 mg, 4.5 mmol) in CH_2Cl_2 (15 mL) was vigorously stirred at ambient temperature for 6 h. The mixture

was extracted with CH_2Cl_2 (150 mL) and saturated NH_4Cl (100 mL), and the aqueous layer was extracted with CH_2Cl_2 (3 × 50 mL). The combined organic layer was dried over anhydrous Na_2SO_4 and concentrated. The residue was purified by chromatography on silica gel column (CH_2Cl_2/MeOH = 25:1) to afford the product **9** (870.0 mg, 88.8%) as a blue solid. ^{1}H NMR (500 MHz, $CDCl_3$): δ 8.64 – 8.61 (d, *J* = 14.4 Hz, 1H), 7.61 (s, 1H), 7.54 – 7.53 (d, *J* = 7.2 Hz, 1H), 7.48 – 7.37 (m, 6H), 7.04 – 7.03 (d, *J* = 8.5 Hz, 2H), 6.98 (s, 1H), 6.49 – 6.46 (d, *J* = 14.5 Hz, 1H), 5.49 – 5.45 (m, 2H), 5.22 (s, 2H), 5.16 (s, 2H), 5.13 – 5.08 (m, 2H), 4.48 (s, 2H), 4.23 – 4.19 (dd, *J* = 11.0, 6.6 Hz, 1H), 4.16 – 4.08 (m, 2H), 3.14 – 3.13 (d, *J* = 7.0 Hz, 2H), 2.77 – 2.72 (d, *J* = 22.2 Hz, 4H), 2.46 (s, 2H), 2.15 (s, 4H), 2.12 – 2.10 (m, 2H), 2.06 (s, 3H), 2.04 (s, 3H), 2.00 (s, 3H), 1.92 (m, 2H), 1.82 (s, 6H), 1.08 – 1.05 (t, *J* = 7.2 Hz, 3H). HRMS (ESI) Calcd for $[C_{55}H_{61}IN_2O_{14}, M\text{-}I]^+$: 973.4117, Found: 973.4483.

(E)-2-(2-(7-(((ethylcarbamoyl)oxy)methyl)-6-((4-((3,4,5-trihydroxy-6-(hydroxymethyl)tetrahydro-2H-pyran-2-yl)oxy)benzyl)oxy)-2,3-dihydro-1H-xanthen-4-yl)vinyl)-3,3-dimethyl-1-(pent-4-yn-1-yl)-3H-indolium iodide (10)

The compound **9** (400 mg, 0.4 mmol) was dissolved in methanol (20 mL). Sodium methoxide (105.3 mg, 1.95 mmol) was added, and the solution was stirred at ambient temperature for 30 min. After neutralization with 2N hydrochloric acid, the reaction mixture was purified by preparative RP-HPLC on a C18 column to afford the product **10** (260.3 mg, 71.8%) as a blue solid. ^{1}H NMR (500 MHz, CD_3OD): δ 8.74 – 8.71 (d, *J* = 14.7 Hz, 1H), 7.69 – 7.67 (d, *J* = 7.4 Hz, 1H), 7.58 – 7.52 (m, *J* = 15.3, 7.5 Hz, 2H), 7.48 – 7.43 (m, 4H), 7.36 (s, 1H), 7.17 – 7.13 (m, 3H), 6.57 – 6.54 (d, *J* = 14.8 Hz, 1H), 5.24 (s, 2H), 5.14 (s, 2H), 4.46 – 4.43 (t, *J* = 7.4 Hz, 2H), 3.91 – 3.90 (d, *J* = 3.2 Hz, 1H), 3.81 – 3.79 (dd, *J* = 9.6, 7.8 Hz, 1H), 3.77 – 3.75 (m, *J* = 5.9, 2.6 Hz, 2H), 3.69 – 3.66 (m, 1H), 3.59 – 3.54 (dd, *J* = 9.7, 3.3 Hz, 1H), 3.18 – 3.13 (q, *J* = 7.2 Hz, 2H), 2.77 – 2.70 (dt, *J* = 24.3, 5.6 Hz, 4H), 2.57 – 2.56 (t, *J* = 2.3 Hz, 1H), 2.43 – 2.40 (m, *J* = 6.5, 2.4 Hz, 2H), 2.11 – 2.06 (m, 2H), 1.93 – 1.91 (m, 2H), 1.84 (s, 6H), 1.13 – 1.10 (t, *J* = 7.2 Hz, 3H). HRMS (ESI) Calcd for $[C_{47}H_{53}IN_2O_{10}, M\text{-}I]^+$: 805.3695, Found: 805.3663.

Gal-Cy-Gd-1

A solution of the compound **10** (20.0 mg, 21.4 μmol), **5** (22.0 mg, 32.1 μmol), $CuSO_4$ (1.6 mg, 6.4 μmol), ascorbic acid (5.1 mg, 25.7 μmol), DMF (0.5 mL), and H_2O (0.2 mL) was stirred at ambient temperature for 4 h. After concentrated *in vacuo*, the reaction mixture was purified by preparative RP-HPLC on a C18 column to afford the product **Gal-Cy-Gd-1** (16.0 mg, 51.1%) as blue solid. HRMS (ESI) Calcd for $[C_{67}H_{85}GdIN_{11}O_{18}, M\text{-}I]^+$: 1489.5315, Found: 1489.5238.

Synthesis of Cy-Gd-1

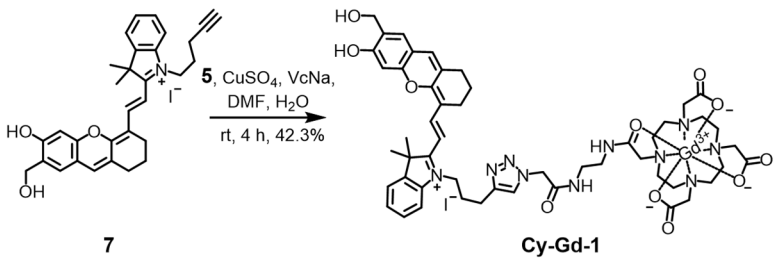

7 **Cy-Gd-1**

Scheme S2. Synthetic routes of Cy-Gd-1.

Cy-Gd-1

A solution of the compound **7** (5.0 mg, 10.7 μmol), **5** (8.8 mg, 12.9 μmol), $CuSO_4$ (0.8 mg, 3.2 μmol), ascorbic acid (2.5 mg, 12.8 μmol), DMF (0.5 mL), and H_2O (0.2 mL) was stirred at ambient temperature for 4 h. After concentrated *in vacuo*, the reaction mixture was purified by preparative RP-HPLC on a C18 column to afford the product **Cy-Gd-1** (5.8 mg, 42.3%) as blue solid. HRMS (ESI) Calcd for $[C_{51}H_{64}GdIN_{10}O_{11}, M\text{-}I]^+$: 1150.3992, Found: 1150.4862.

2.2. Synthesis of Gal-Cy-Gd-2

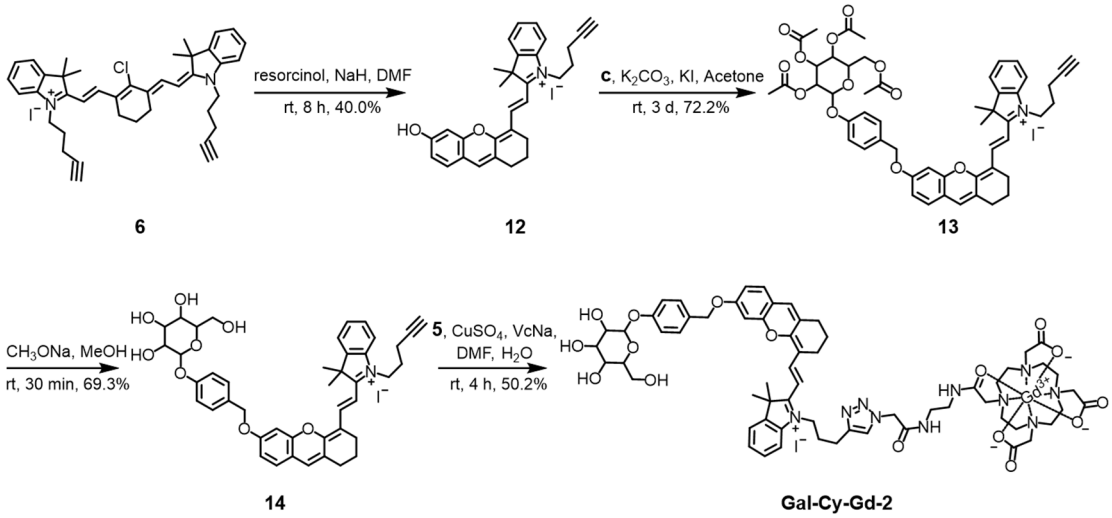

Scheme S3. Synthetic routes of Gal-Cy-Gd-2

(E)-2-(2-(6-hydroxy-2,3-dihydro-1H-xanthen-4-yl)vinyl)-3,3-dimethyl-1-(pent-4-yn-1-yl)-3H-indolium iodide (12)

To a solution of resorcinol (924.9 mg, 8.4 mmol), NaH (336.0 mg, 8.4 mmol) in DMF (10 mL), a solution of the compound **6** (3.0 g, 4.2 mmol) in DMF (10 mL) was added, and the reaction was stirred at ambient temperature for 8 h. Then the mixture was concentrated and extracted with CH_2Cl_2 (150 mL) and saturated NH_4Cl (100 mL), and the aqueous layer was extracted with CH_2Cl_2 (3 × 50 mL). The combined organic layer was dried over anhydrous Na_2SO_4 and concentrated. The residue was purified by chromatography on silica gel column (CH_2Cl_2/MeOH = 100:3) to afford the product **12** (1.0 g, 40.0%) as blue solid. ^1H NMR (500 MHz, $CDCl_3$): δ 8.54 (d, *J* = 13.7 Hz, 1H), 7.38 – 7.34 (m, 2H), 7.23 – 7.17 (m, 5H), 6.92 – 6.90 (d, *J* = 8.1 Hz, 1H), 6.16 – 6.13 (d, *J* = 13.2 Hz, 1H), 4.20 (s, 2H), 2.66 (s, 2H), 2.57 (s, 2H), 2.33 (s, 2H), 2.10 (s, 1H), 2.01 (s, 2H), 1.84 (s, 2H), 1.71 – 1.70 (d, *J* = 1.8 Hz, 6H). HRMS (ESI) Calcd for $[C_{30}H_{30}INO_2, M\text{-}I]^+$: 436.2271, Found: 436.2829.

(E)-3,3-dimethyl-1-(pent-4-yn-1-yl)-2-(2-(6-((4-((3,4,5-triacetoxy-6-(acetoxymethyl)tetrahydro-2H-pyran-2-yl)oxy)benzyl)oxy)-2,3-dihydro-1H-xanthen-4-yl)vinyl)-3H-indolium iodide (13)

A solution of the compound **12** (1.0 g, 1.8 mmol), **c** (1.1 g, 2.1 mmol), KI (581.0 mg, 3.5 mmol) and K_2CO_3 (290.2 mg, 2.1 mmol) in acetone (20 mL) was vigorously stirred at ambient temperature for 3 d. The mixture was extracted with CH_2Cl_2 (200 mL) and saturated NH_4Cl (150 mL), and the aqueous layer was extracted with CH_2Cl_2 (3 × 100 mL). The combined organic layer was dried over anhydrous Na_2SO_4 and concentrated. The residue was purified by chromatography on silica gel column (CH_2Cl_2/MeOH = 100:3) to afford the product **13** (1.3 g,

72.2%) as a blue solid. ^{1}H NMR (500 MHz, $CDCl_3$): δ 8.68 – 8.65 (d, *J* = 14.7 Hz, 1H), 7.51 – 7.45 (m, 2H), 7.42 – 7.38 (m, 5H), 7.27 (s, 1H), 7.05 – 7.04 (d, *J* = 8.5 Hz, 2H), 6.98 – 6.95 (m, 2H), 6.49 – 6.46 (d, *J* = 14.7 Hz, 1H), 5.50 – 5.45 (m, 2H), 5.15 – 5.11 (m, 3H), 5.09 – 5.07 (d, *J* = 7.9 Hz, 1H), 4.44 – 4.41 (t, *J* = 7.3 Hz, 2H), 4.23 – 4.20 (dd, *J* = 11.2, 6.9 Hz, 1H), 4.17 – 4.13 (dd, *J* = 11.3, 6.3 Hz, 1H), 4.09 – 4.07 (t, *J* = 6.6 Hz, 1H), 2.75 – 2.73 (m, 2H), 2.69 – 2.67 (t, *J* = 5.9 Hz, 2H), 2.41 – 2.38 (td, *J* = 6.4, 2.3 Hz, 2H), 2.16 (s, 3H), 2.14 – 2.13 (t, *J* = 2.5 Hz, 1H), 2.11 – 2.08 (m, 2H), 2.06 – 2.04 (d, *J* = 7.4 Hz, 6H), 2.00 (s, 3H), 1.93 – 1.90 (m, 2H), 1.79 (s, 6H). HRMS (ESI) Calcd for $[C_{51}H_{54}INO_{12}, M\text{-}I]^+$: 872.3641, Found: 872.4426.

(E)-3,3-dimethyl-1-(pent-4-yn-1-yl)-2-(2-(6-((4-((3,4,5-trihydroxy-6-(hydroxymethyl)tetrahydro-2H-pyran-2-yl)oxy)benzyl)oxy)-2,3-dihydro-1H-xanthen-4-yl)vinyl)-3H-indolium iodide (14)

The compound **13** (400 mg, 0.4 mmol) was dissolved in methanol (20 mL). Sodium methoxide (108.0 mg, 2.0 mmol) was added, and the solution was stirred at ambient temperature for 30 min. After neutralization with 2N hydrochloric acid, the reaction mixture was purified by preparative RP-HPLC on a C18 column to afford the product **14** (230.6 mg, 69.3%) as a blue solid. ^{1}H NMR (500 MHz, CD_3OD): δ 8.78 – 8.75 (d, *J* = 14.8 Hz, 1H), 7.68 – 8.66 (d, *J* = 7.3 Hz, 1H), 7.57 – 7.51 (ddd, *J* = 11.5, 9.0, 4.4 Hz, 2H), 7.48 – 7.40 (m, 5H), 7.17 – 7.15 (m, 2H), 7.09 (d, *J* = 2.2 Hz, 1H), 7.05 – 7.03 (dd, *J* = 8.6, 2.4 Hz, 1H), 6.58 – 6.55 (d, *J* = 14.8 Hz, 1H), 5.20 (s, 2H), 4.89 (s, 1H), 4.46 – 4.43 (t, *J* = 7.4 Hz, 2H), 3.91 – 3.90 (d, *J* = 3.2 Hz, 1H), 3.82 – 3.73 (m, 3H), 3.70 – 3.68 (m, 1H), 3.59 – 3.57 (dd, *J* = 9.7, 3.4 Hz, 1H), 2.79 – 2.71 (dt, *J* = 26.1, 5.9 Hz, 4H), 2.56 – 2.55 (t, *J* = 2.6 Hz, 1H), 2.43 – 2.40 (td, *J* = 6.5, 2.6 Hz, 2H), 2.11 – 2.06 (m, 2H), 1.96 – 1.91 (m, 2H), 1.83 (s, 6H). HRMS (ESI) Calcd for $[C_{43}H_{46}INO_8, M\text{-}I]^+$: 704.3218, Found: 704.3247.

Gal-Cy-Gd-2

A solution of the compound **14** (20.0 mg, 24.0 μmol), **5** (19.8 mg, 28.8 μmol), $CuSO_4$ (1.8 mg, 7.2 μmol), ascorbic acid (5.5 mg, 28.8 μmol), DMF (0.5 mL), and H_2O (0.2 mL) was stirred at ambient temperature for 4 h. After concentrated *in vacuo*, the reaction mixture was purified by preparative RP-HPLC on a C18 column to afford the product **Gal-Cy-Gd-2** (18.3 mg, 50.2%) as blue solid. HRMS (ESI) Calcd for $[C_{63}H_{78}GdIN_{10}O_{16}, M\text{-}I]^+$: 1388.4833, Found: 1388.4818.

Synthesis of Cy-Gd-2

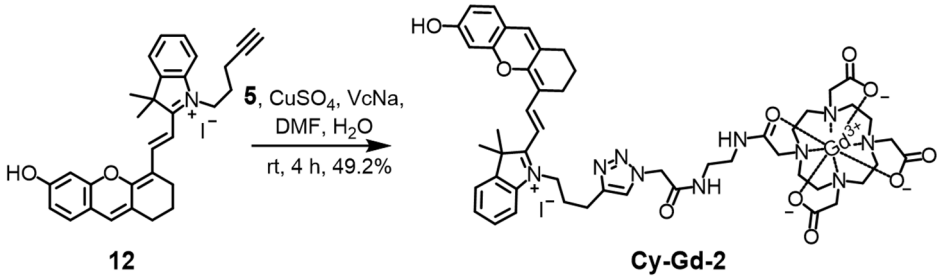

12 **Cy-Gd-2**

Scheme S4. Synthetic routes of Cy-Gd-2

Cy-Gd-2

A solution of the compound **12** (6.0 mg, 10.6 μmol), **5** (8.7 mg, 12.8 μmol), $CuSO_4$ (0.8 mg, 3.2 μmol), ascorbic acid (2.5 mg, 12.8 μmol), DMF (0.5 mL), and H_2O (0.2 mL) was stirred at ambient temperature for 4 h. After concentrated *in vacuo*, the reaction mixture was purified by preparative RP-HPLC on a C18 column to afford

the product **Cy-Gd-2** (6.5 mg, 49.2%) as blue solid. HRMS (ESI) Calcd for $[C_{51}H_{64}GdIN_{10}O_{11}, M\text{-}I]^+$: 1120.3886, Found: 1120.4727.

3. Determination of the Sensitivity of Gal-Cy-Gd-1 towards *β*-gal

Gal-Cy-Gd-1 (5 μM) and *β*-gal (2 U/mL) were incubated at varying times (0, 5, 10, 15, 20, 25, 30, 40, 50, 60, 70, 80, 90 min) in PBS buffer (pH 7.4) at 37 ºC. An EVOLUTION-220 UV−vis spectrometer measured the UV absorption at 400-800 nm, and the fluorescence spectra were then recorded on an Edinburgh FS5 fluorescence spectrometer, with an excitation at 685 nm.

Gal-Cy-Gd-1 (5 μM) was incubated with varying concentrations of *β*-gal (0, 0.05, 0.1, 0.2, 0.4, 0.6, 0.8, 1.0 and 2.0 U/mL) in PBS buffer (pH 7.4) at 37 ºC for 90 min, and the fluorescence spectra were then recorded on an Edinburgh FS5 fluorescence spectrometer, with an excitation at 685 nm.

4. Determination of the Specificity towards *β*-gal

The specificity towards *β*-gal *in vitro* was evaluated based on two modalities of fluorescence and MRI, respectively. First, Gal-Cy-Gd-1 (5 μM) in PBS buffer was incubated with 2 U/mL of trypsin, 10 mg/mL of BSA, 30 mg/L of GSH, 2 U/mL of NTR, 2 U/mL of lysozyme, 2 U/mL of *β*-gal or 2 U/mL of *β*-gal pretreated with its inhibitor, D-(+)-ribonucleic acid-lactone (15 mg/mL) for 30 min. The solutions were kept at 37 ºC for 90 min. The fluorescence spectra were then acquired with an excitation at 685 nm. Second, Gal-Cy-Gd-1 (300 μM) in PBS buffer was incubated with 100 U/mL of trypsin, 40 mg/mL of BSA, 0.2 mg/mL of GSH, 100 U/mL of NTR, 100 U/mL of lysozyme, 100 U/mL of *β*-gal or 100 U/mL of *β*-gal pretreated with its inhibitor, D-(+)-ribonucleic acid-lactone (100 mg/mL) for 30 min. The solutions were kept at 37 ºC for 90 min. The T_1 value in each solution was then acquired by a series of inversion-prepared fast spin−echo scans on the 0.5 T MR scanner (Bruker, Germany).

5. Measurement of the Longitudinal Relaxivity r_1

To measure the r_1 relaxivities of Gal-Cy-Gd-1 or Gal-Cy-Gd-2, a series of PBS buffers containing 0.1, 0.2, 0.3 and 0.4 mM of Gal-Cy-Gd-1 or Gal-Cy-Gd-2 were prepared. To measure the r_1 relaxivities of Gal-Cy-Gd-1 or Gal-Cy-Gd-2 following activation by *β*-gal, various concentrations of Gal-Cy-Gd-1 or Gal-Cy-Gd-2 (0.1, 0.2, 0.3 and 0.4 mM) in PBS buffer (pH 7.4) were incubated with 40 U/mL *β*-gal at 37 ºC for 90 min, respectively. And various concentrations of Gal-Cy-Gd-1 or Gal-Cy-Gd-2 (0.1, 0.2, 0.3 and 0.4 mM) in PBS buffer (pH 7.4) were incubated with 40 U/mL *β*-gal and BSA (0.6 mM) at 37 ºC for 90 min, respectively.

Then, each solution's T_1 value was acquired on a 20 MHz MR scanner (Bruker, Germany), using a series of inversion-prepared fast spin−echo scans. Relaxation rates (R_1) were determined as $1/T_1$, which were plotted versus the concentrations of each probe. The plot was fitted by linear regression, and the longitudinal molar relaxivities (r_1, unit of $mM^{-1}\ s^{-1}$) were calculated based on the slope of each plot.

6. SDS-PAGE

Gal-Cy-Gd-1 (100 μM) and Gal-Cy-Gd-2 (100 μM) were incubated with *β*-gal (500 $\mu g \cdot mL^{-1}$) in PBS buffer (pH 7.4) at 37 ºC for 90 min, respectively. Samples were treated with SDS and *β*-mercaptoethanol, vortexed, heated at 100 °C for 5 min, and loaded on the gel. After the electrophoresis, a fluorescence image was taken with a digital camera under illumination at 680 nm from BIO-Red. After the fluorescence image had been taken, the gel was stained with Coomassie brilliant blue, and an image of the stained gel was taken.

7. MR Imaging of Gd-based Probes

Gal-Cy-Gd-1 (0.3 mM) in PBS buffer (pH 7.4) were incubated with 40 U/mL *β*-gal or 40 U/mL *β*-gal and BSA (0.6 mM) at 37 ºC for 90 min, respectively.

The T_1 values were measured by a 9.4 T MR scanner (Bruker, Germany) using the T_1-weighted Multi-Slice Multi Echo (MSME) sequence with an echo time (TE) of 5.5 ms and a repetition time (TR) of 600.0 ms.

8. Cell Experiments

8.1. Cell Culture Conditions

SKOV3 cells or 293T cells were cultured in high-glucose DMEM (Cell-Box) medium containing 10% fetal bovine serum (FBS) and 1% penicillin/streptomycin (PS) in 5% CO_2 humidified atmosphere (95%) at 37 °C.

8.2. Cell Viability Assays

The cytotoxicity of Gal-Cy-Gd-1 or Gal-Cy-Gd-2 to SKOV3 cells was evaluated by CCK8 (Cell Counting Kit-8) Cell Proliferation and Cytotoxicity assay following the manufacturer's protocol. In brief, cells (1×10^4 cells/well) in DMEM (supplemented with 10% FBS, 200 μL) were seeded in 96-well plate and incubated at 37 °C overnight. The medium was then changed and cells were treated with Gal-Cy-Gd-1 or Gal-Cy-Gd-2 at a serial of concentrations (0, 2, 5, 10, 25, 50 and 100 μM) in FBS-free DMEM (100 μL) at 37 °C with 5% CO_2 and 95% humidity for 24 h. After the removal of the medium, FBS-free DMEM (90 μL) supplemented with CCK8 (10 μL, 1 × 100 T) was added to each well and incubated at 37 °C with 5% CO_2 and 95% humidity for 2 h. Absorbance at 450 nm was measured with a microplate reader and cell viability was calculated based on untreated wells. Each experiment was triplicated.

8.3. Fluorescence Imaging of Cells

SKOV3 cells were incubated with Gal-Cy-Gd-1 (10 μM) in FBS-free DMEM at various time (1 h, 2 h, 4 h, 6 h and 8 h). The culture medium was removed and the cells were washed three times with PBS and the fluorescence images were captured with a fluorescence microscope (Nikon, Japan)

Cells were dispersed onto a glass-bottom dish (8×10^4 cells) (Cellvis, D35-20-1-N, 35 mm Dish with 20 mm bottom Well) and allowed to grow overnight. Gal-Cy-Gd-1 or Gal-Cy-Gd-2 (10 μM) in FBS-free DMEM was added into dishes and incubated in 5% CO_2 humidified atmosphere at 37 ºC for 6 h. For the inhibition experiments, cells were pretreated with *β*-gal inhibitor D-(+)-ribonucleic acid-lactone (15 mg/mL) for 30 min before incubation with Gal-Cy-Gd-1 (10 μM) for 6 h. The culture medium was removed and the cells were washed three times with PBS. After adding PBS, Cell images were taken using a fluorescence microscope (Nikon, Japan), with excitation/emission at Cy5.5 channel.

8.4. Flow Cytometry

SKOV3 cells (1×10^5 cells per sample) were incubated in a glass-bottom dish containing Gal-Cy-Gd-1 or Gal-Cy-Gd-2 (10 μM) at 37 °C with 5% CO_2 and 95% humidity for 6 h. After being washed with PBS, cells were transferred in a microcentrifuge tube and then resuspended in PBS (100 μL). The fluorescence of cell samples was analyzed with a flow cytometer (CytoFLEX S, 16 Beckman and NovoCyte Advanteon).

9. Animals and Tumor Models

All experimental protocols involving animals were approved by the Animal Welfare and Research Ethics Committee at Innovation Academy for Precision Measurement Science and Technology, Chinese Academy of Sciences (APM23024T). BALB/c female mice at 4-5 weeks old were purchased from the Wuhan Bainte Biotechnology Co., Ltd. Mice were housed at 25 °C with free access to food and water. Xenograft tumor model mice was established by subcutaneous injection of 2 × 10^6 SKOV3 cells suspended in 100 μL PBS. The tumors were allowed to grow for around 4-5 weeks to reach the size of about 100-200 mm^3 before being used for fluorescence and MR imaging.

To establish an orthotropic ovarian cancer model, 1 × 10^5 SKOV3-luciferase-transfected (Luci-SKOV3) cells in a total volume of 10 μL PBS were directly injected into the left ovary under anesthesia by pentobarbital sodium.[2] Bioluminescent imaging (BLI) was used to monitor mouse tumor growth and development. One month later, the orthotropic ovarian tumors were successfully established.

10. Fluorescence Imaging of *β*-gal Activity in Mice

To investigate the accumulation of these probes to *β*-gal-overexpressing-tumor, mice were injected through the tail vein with Gal-Cy-Gd-1 or Gal-Cy-Gd-2 (0.5 μmol kg^{-1}) in 100 μL PBS. Whole body fluorescence images were acquired before injection, as well as 1 h, 2 h, 4 h, 8 h, 12 h, 24 h, 48 h and 72 h post-injection.

For fluorescence imaging in living mice bearing orthotropic SKOV3/Luc tumors, mice were i.v. injected with Gal-Cy-Gd-1 (0.5 μmol kg^{-1}) in 100 μL PBS. Then fluorescence images were acquired before injection and 10 h post-injection.

The whole-body fluorescence images were acquired on an IVIS Lumina XRMS Series III imaging system at indicated time point with an excitation wavelength of 710 nm and an emission wavelength of 760 nm. The ROIs measurement measured using Living Image Software (PerkinElmer, U.S.A) quantified the fluorescence intensities. Each experiment was conducted in three mice.

11. MR imaging of *β*-gal in mice

For T_1-weighted MR imaging of *β*-gal activity in living mice bearing subcutaneous SKOV3 tumors, mice were i.v. injected with Gal-Cy-Gd-1 or Gal-Cy-Gd-2 (0.02 mmol kg^{-1} Gd^{3+}) in 100 μL PBS. The MR imaging was acquired before injection, 2 h, 4 h, 6 h and 8 h post-injection. For non-invasive MR imaging of *β*-gal activity in living mice bearing orthotropic SKOV3/Luc tumors, mice were i.v. injected with Gal-Cy-Gd-1 (0.02 mmol kg^{-1} Gd^{3+}) in 100 μL PBS. Then, the T_1-weighted MR images were acquired before injection and 4 h post-injection. All the MR imaging experiments were conducted on a 9.4 T MR scanner (Bruker, Germany). The mice were scanned in the tail-first prone position. For the subcutaneous SKOV3 tumor model and orthotropic ovarian tumor modal, the images were acquired using a T_1-RARE imaging sequence. The detailed MR imaging parameters were as follows: repetition time ms/echo time ms, 600/6 ms; image size, 256 × 256; slice thickness 0.8 mm; slices, 12; field of view, 35 mm × 35 mm. The acquisition time for each MR imaging was 10 min 55 s. Each experiment was conducted in three mice. Acquired MRI data were then transferred as DICOM images to a RadiAnt DICOM Viewer for quantitative image analysis. This consisted of manual segmentation of the tumor ROI for each slice, slice-wise normalization of mean tumor signal intensity with the water reference standard to account for inter-session variability, followed by combining these normalized, slice-wise values to generate mean volumetric tumor signal intensities (SI) for each time point. Percentage signal enhancement (% SE) was calculated at each time point as the % difference between the tumor SI in the precontrast data set: % SE (t) = (SI (t) - SI (t = 0))/SI (t = 0); for each mouse, for every session.

12. Fluorescence Imaging of Tumors and Main Organs *ex vivo*

SKOV3 tumor-bearing mice were i.v. injected with Gal-Cy-Gd-1 or Gal-Cy-Gd-2 (0.5 μmol kg^{-1}) in 100 μL PBS. After 72 h, mice were sacrificed. Tumors and main organs were resected, including the heart, liver, spleen, lung, and kidneys. The fluorescence images of these organs and tumors were acquired with the IVIS Lumina XRMS Series III imaging system using a 710 nm excitation filter and a 760 nm emission filter. Each experiment was conducted in three mice.

13. Biodistribution Studies

SKOV3 tumor-bearing mice were i.v. injected with Gal-Cy-Gd-1 or Gal-Cy-Gd-2 (0.02 mmol kg^{-1} Gd^{3+}) in 100 μL PBS (n = 3 per group). After being sacrificed at 4 h, tumors and major organs including liver, kidneys, heart, lung, and spleen were collected and weighed. The tissues were cut into small pieces and digested with concentrated HNO_3 under heating at 120 ºC overnight. The residue in each organ was then diluted with 5 mL 2% HNO_3 solution, and the concentration of Gd^{3+} was determined by ICP-MS. The %ID/g was also calculated for comparison.

14. Fluorescence Image-guided Surgery

SKOV3/Luc tumor-bearing mice were anesthetized, and their respiration and body temperature were constantly monitored. For the fluorescence image-guided surgery group, 100 μM Gal-Cy-Gd-1 in 100 μL PBS was i.v. injected. The fluorescence images were acquired after 10 h, which was used to guide surgical resection of tumor tissues from the ovarian. Bioluminescence imaging was applied before and after surgery to detect the tumor residuals.

15. Statistical Analysis

Results are expressed as the mean ± standard deviation unless otherwise stated. Student's t-test determined the statistical comparison between the two groups. $P < 0.05$ was considered statistically significant. All statistical calculations were performed using Origin Pro 8.5.

16. Dynamic Calculation Method

To evaluate the binding affinities between the probes and *β*-gal, the molecular docking calculations were carried out on AutoDock Vina software (1.2.0 version).[3] The crystal structure of *β*-gal was obtained from the protein data bank (www.pdb.org) under code 1JYN, and the initial geometry models of the probes were generated by quantum chemical calculations with PM6 method performed on Gaussian09 software.[4] The figures of the docking modes are obtained by PyMol and LigPlot+.

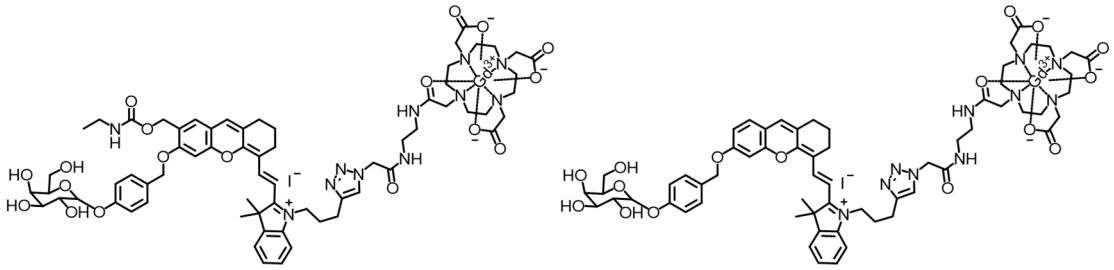

Gal-Cy-Gd-1 Gal-Cy-Gd-2

Fig. S1. The chemical structure of Gal-Cy-Gd-1 and Gal-Cy-Gd-2.

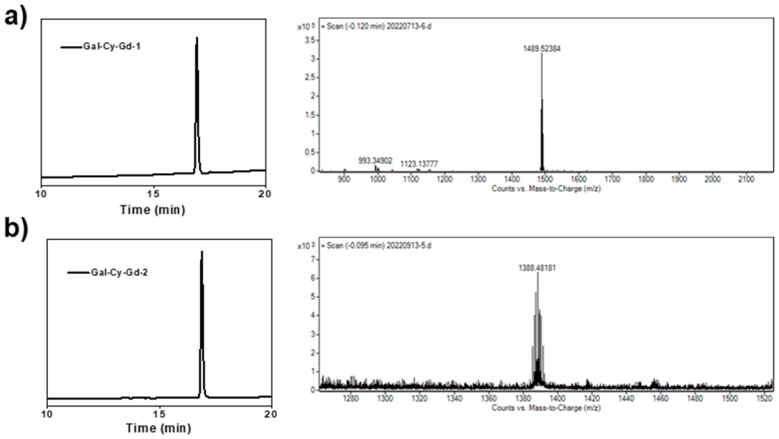

Fig. S2. HPLC spectra and mass spectra for (a) Gal-Cy-Gd-1 and (b) Gal-Cy-Gd-2.

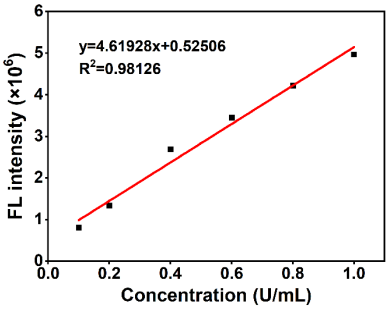

Fig. S3. The linear fitting curve of fluorescence intensity (λ_{em} = 717 nm) with the concentration of *β*-gal from 0.1 - 1.0 U/mL. The detection limit was found to be 0.068 U/mL, using a 3σ/k method.

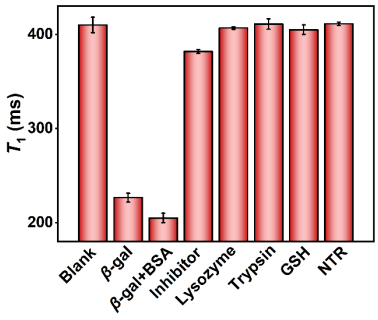

Fig. S4. T_1 values of Gal-Cy-Gd-1 incubated with trypsin, GSH, NTR, lysozyme, *β*-gal, *β*-gal + BSA, and *β*-gal with its inhibitor in PBS (pH 7.4).

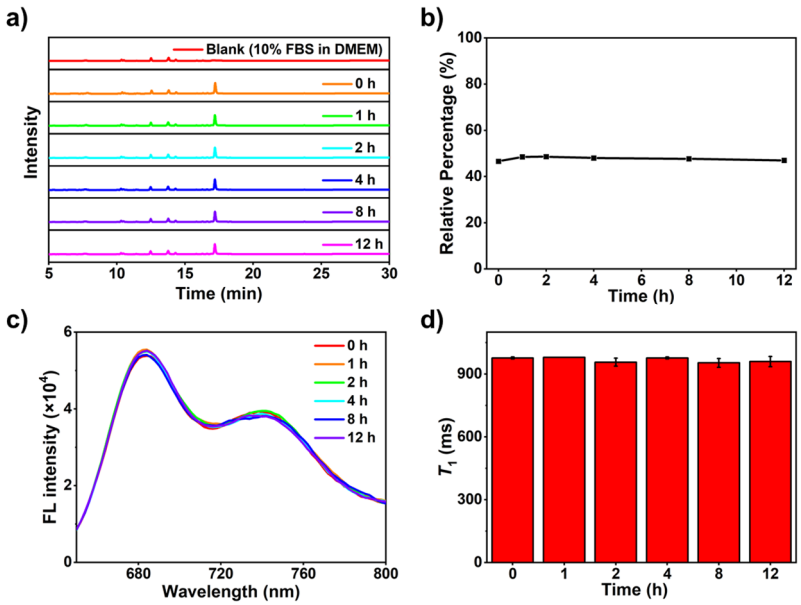

Fig. S5. Stability test of Gal-Cy-Gd-1. Time-dependent (a) HPLC traces, (b) HPLC peak area ratio, (c) fluorescence and (d) T_1 values of Gal-Cy-Gd-1 incubated in DMEM containing 10% FBS for 12 h. (λ_{ex} = 607 nm).

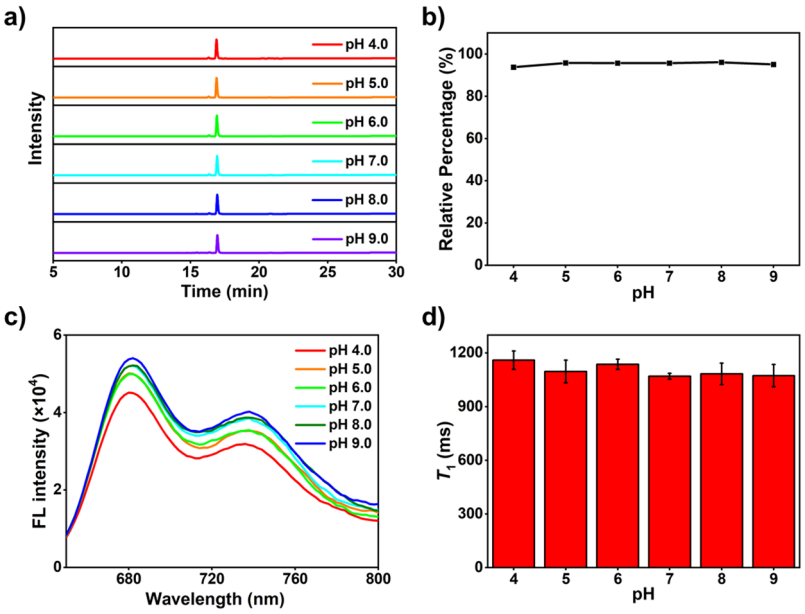

Fig. S6. Stability test of Gal-Cy-Gd-1. (a) HPLC traces, (b) HPLC peak area ratio, (c) fluorescence and (d) T_1 values of Gal-Cy-Gd-1 incubated under different pH value for 4 h. (λ_{ex} = 607 nm).

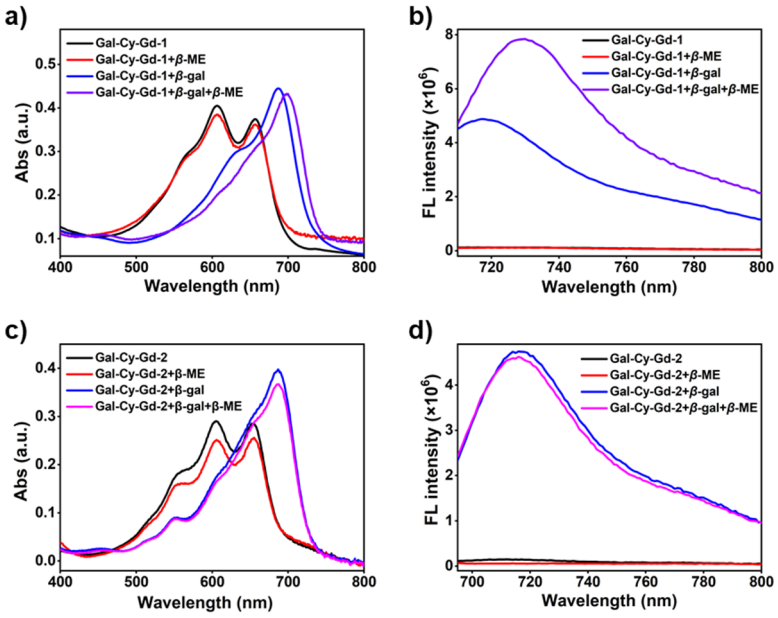

Fig. S7. (a) UV-Vis absorption spectra and (b) fluorescence spectra of Gal-Cy-Gd-1 (5 μM) before and after incubation with β-gal (2 U/mL) in the presence or absence of β-mercaptoethanol (140 mM) in PBS at 37 °C for 2 h. (c) UV-Vis absorption spectra and (d) fluorescence spectra of Gal-Cy-Gd-2 (5 μM) before and after incubation with β-gal (2 U/mL) in the presence or absence of β-mercaptoethanol (140 mM) in PBS at 37 °C for 2 h.

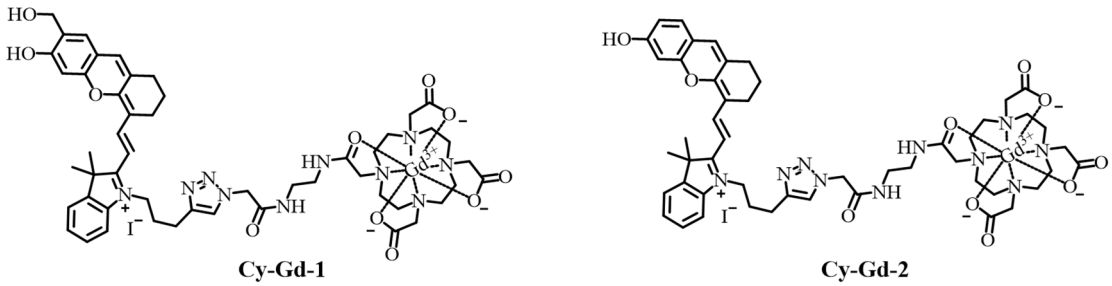

Fig. S8. The chemical structure of Cy-Gd-1 and Cy-Gd-2.

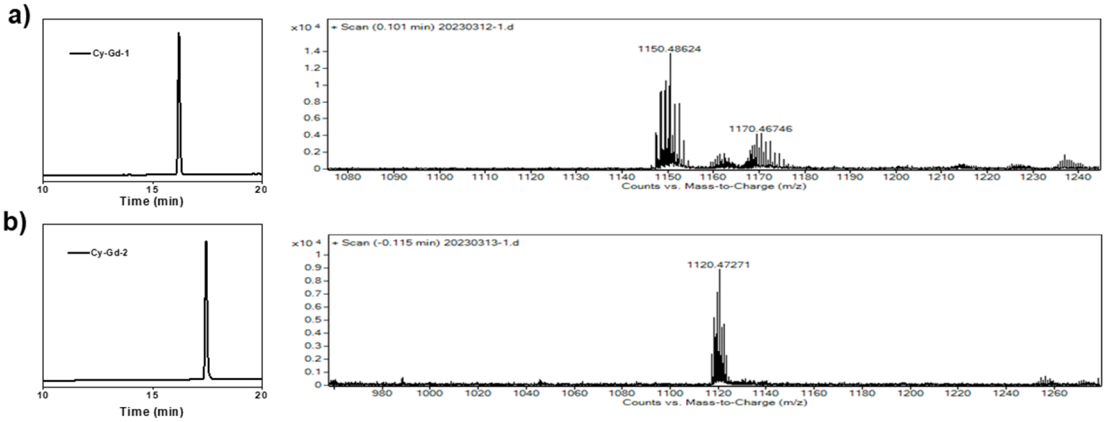

Fig. S9. HPLC spectra and mass spectra for (a) Cy-Gd-1 and (b) Cy-Gd-2.

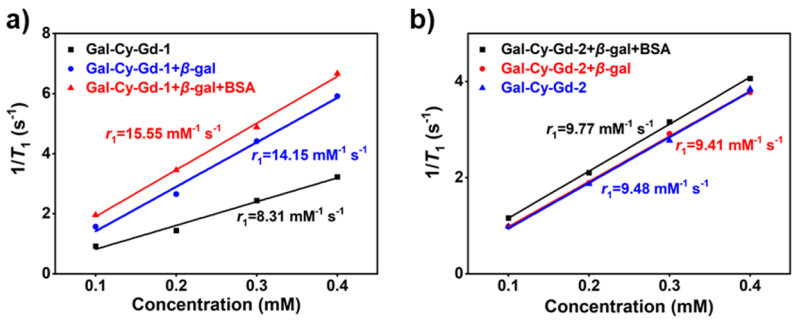

Fig. S10. Plots of $1/T_1$ vs Gd^{3+} concentration to determine the r_1 relaxivities of (a) Gal-Cy-Gd-1 and (b) Gal-Cy-Gd-2. Varying concentrations of each probe (100-400 μM) was dissolved in PBS (pH = 7.4). The resulting solutions were scanned using the standard inversion recovery spin-echo sequence on 20 MHz MR Scanner. The true concentrations of Gd^{3+} in the solutions were further confirmed by ICP-MS measurement. The longitudinal relaxivites (r_1, units of $mM^{-1}s^{-1}$) were determined as the slope of $1/T_1$ (R_1) vs Gd^{3+} concentration. The values are summarized in Table 1. These results show a higher r_1 relaxivity of Gal-Cy-Gd-1 after incubation with *β*-gal but little change of r_1 relaxivity of Gal-Cy-Gd-2 following incubation with *β*-gal.

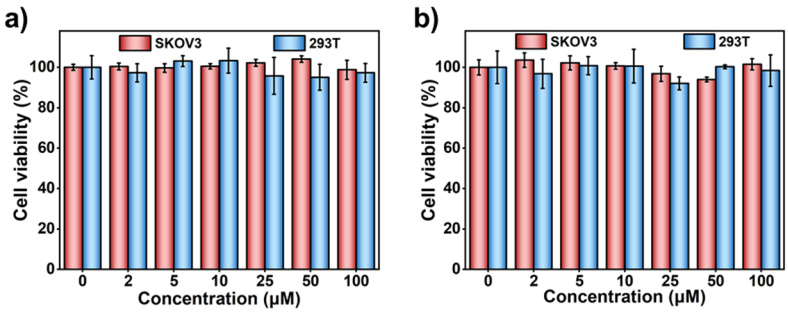

Fig. S11. The cell viability test. Human ovarian cancer cells (SKOV3) or normal human embryonic kidney cells (293T) were incubated with (a) Gal-Cy-Gd-1 and (b) Gal-Cy-Gd-2 at 0, 2, 5, 10, 25, 50 and 100 μM for 24 h, and the cell viability was determined by MTT assay. Data bars show mean ± s.d. (n = 6 technical replicates). These results indicated that Gal-Cy-Gd-1 and Gal-Cy-Gd-2 all exhibit high biocompatibility against two cells.

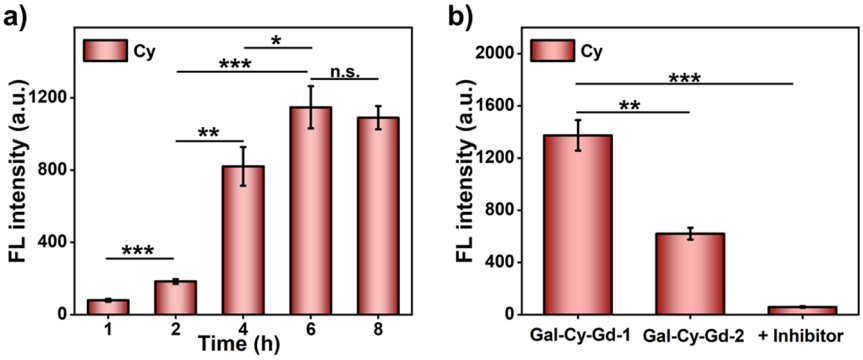

Fig. S12. Imaging of *β*-gal activity in tumor cells. (a) Average intracellular fluorescence intensities at different time points after incubation with Gal-Cy-Gd-1. (b) Average intracellular fluorescence intensities of SKOV3 cells with Gal-Cy-Gd-1 or Gal-Cy-Gd-2 (10 μM) incubated at 37 °C for 6 h, as well as cells pretreated with D-(+)-ribonucleic acid-lactone, an *β*-gal inhibitor, for 30 min before incubation with Gal-Cy-Gd-1. Data bars show mean ± s.d. (n = 3).

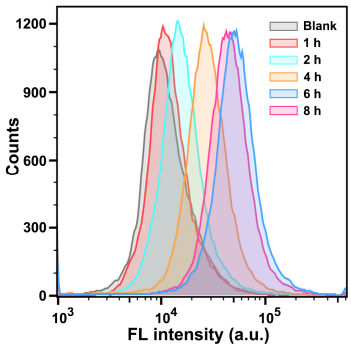

Fig. S13. Flow cytometry of SKOV3 cells incubated with Gal-Cy-Gd-2 (10 μM) at 37 °C for 1−8 h.

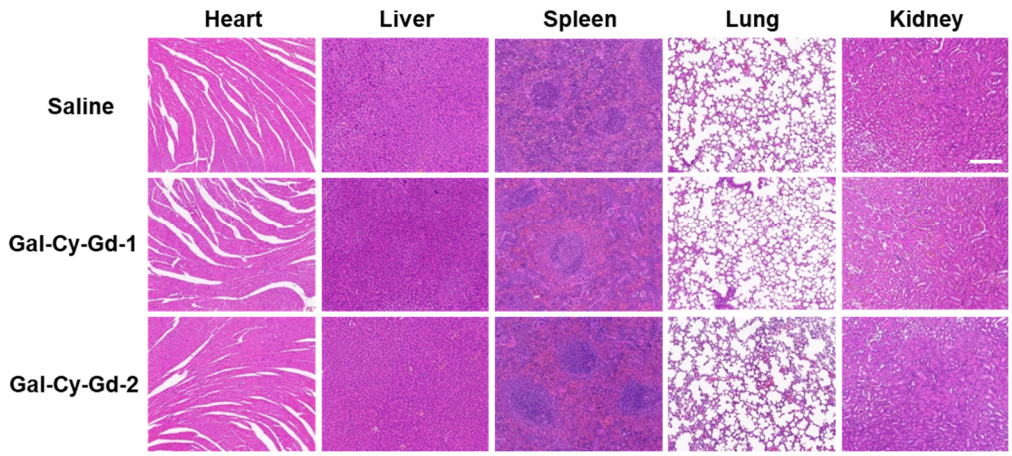

Fig. S14. H&E staining of tissue sections of mice i.v. injected with saline, Gal-Cy-Gd-1 and Gal-Cy-Gd-2. (Scale bar, 200 μm).

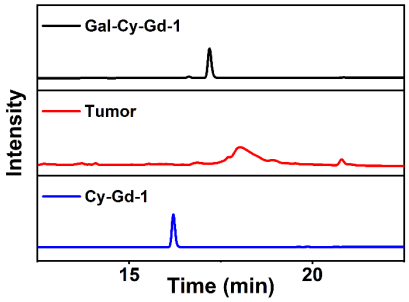

Fig. S15. HPLC trace of Gal-Cy-Gd-1 (black), Cy-Gd-1 (blue), or tumor lysate (red) resected from mice of SKOV3 tumor at 4 h following injection of Gal-Cy-Gd-1 (0.02 mmol kg^{-1} Gd^{3+}, i.v.).

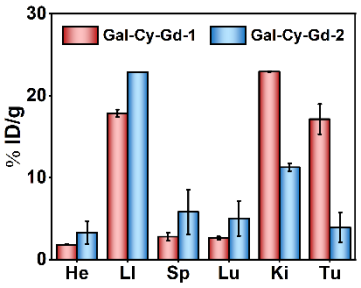

Fig. S16. Biodistribution (% ID/g) of Gal-Cy-Gd-1 (red) or Gal-Cy-Gd-2 (blue) in SKOV3 tumors and main organs (He: heart, Li: liver, Sp: spleen, Lu: lung, Ki: kidneys, Tu: tumor) at 4 h after i.v. injection into mice (0.02 mmol kg^{-1} Gd^{3+}). The amount of Gd^{3+} in tumors and main organs were determined by ICP-MS.

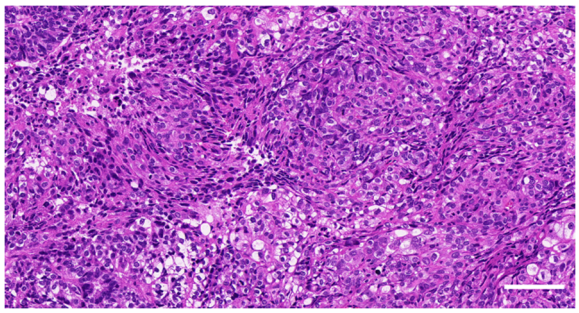

Fig. S17. H&E staining of ovarian cancer *in situ*. Scale bar = 100 μm

Reference:

[1] J.Y. Hyun, N.R. Kang, I. Shin, *Org. Lett.* **2018**, *20*, 1240-1243.

[2] S.A. Belinsky, M.J. Grimes, M.A. Picchi, H.D. Mitchell, C.A. Stidley, Y. Tesfaigzi, M.M. Channell, Y. Liu, R.A. Casero, S.B. Baylin, M.D. Reed, C.S. Tellez, T.H. March, *Cancer Res*. **2011**, *71*, 454-462.

[3] J. Eberhardt, D. Santos-Martins, A.F. Tillack, S. Forli, *J. Chem. Inf. Model.* **2021**, *61*, 3891-3898.

[4] D.H. Juers, T.D. Heightman, A. Vasella, J.D. McCarter, L. Mackenzie, S.G. Withers, B.W. Matthews, *Biochemistry*. **2001**, *40*, 14781-14794.

^{1}H NMR spectra of compound **a** in $CDCl_3$

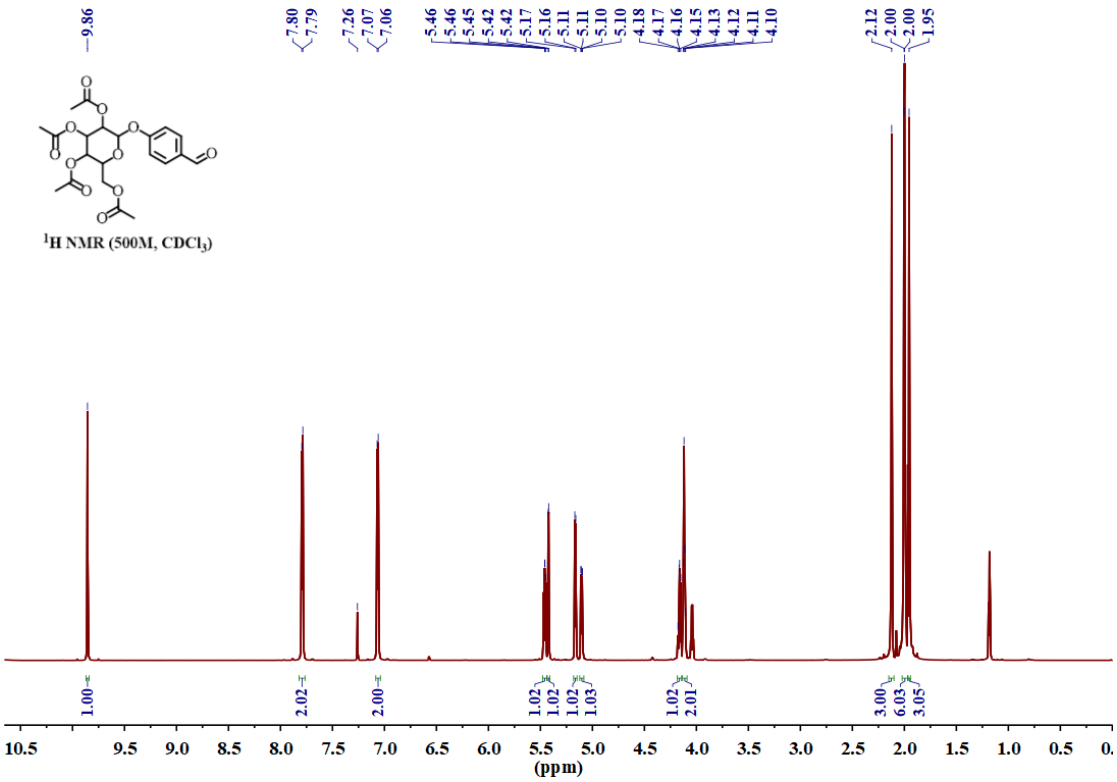

HRMS spectra of compound **a**

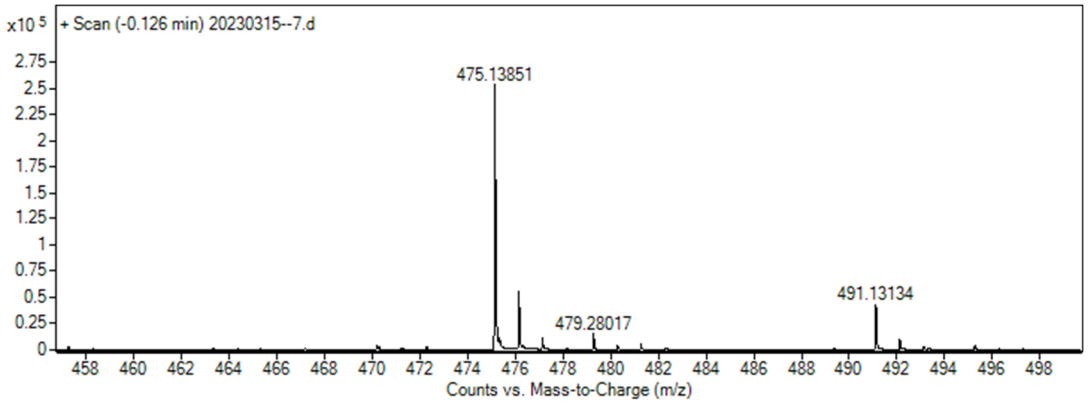

^{1}H NMR spectra of compound **b** in $CDCl_3$

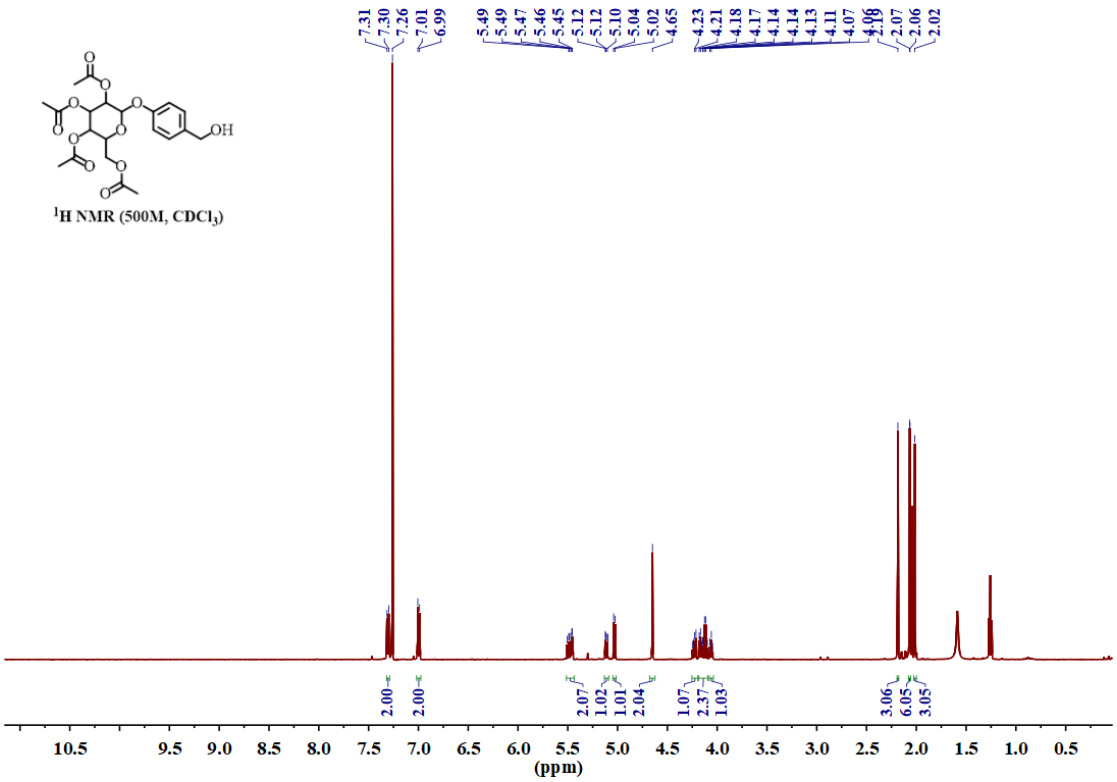

HRMS spectra of compound **b**

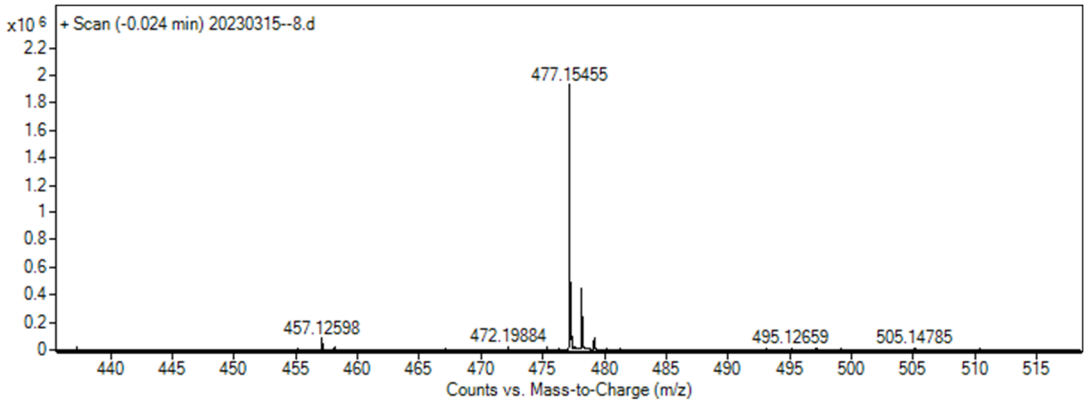

^{1}H NMR spectra of compound **c** in $CDCl_3$

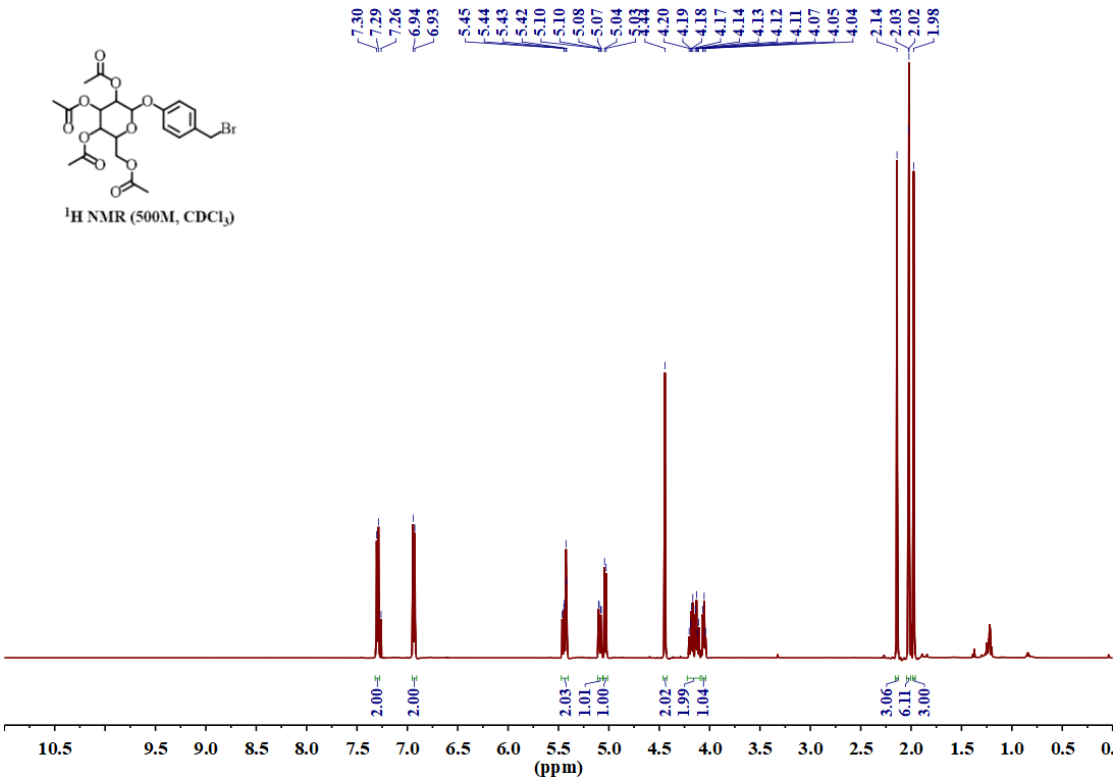

^{13}C NMR spectra of compound **c** in $CDCl_3$

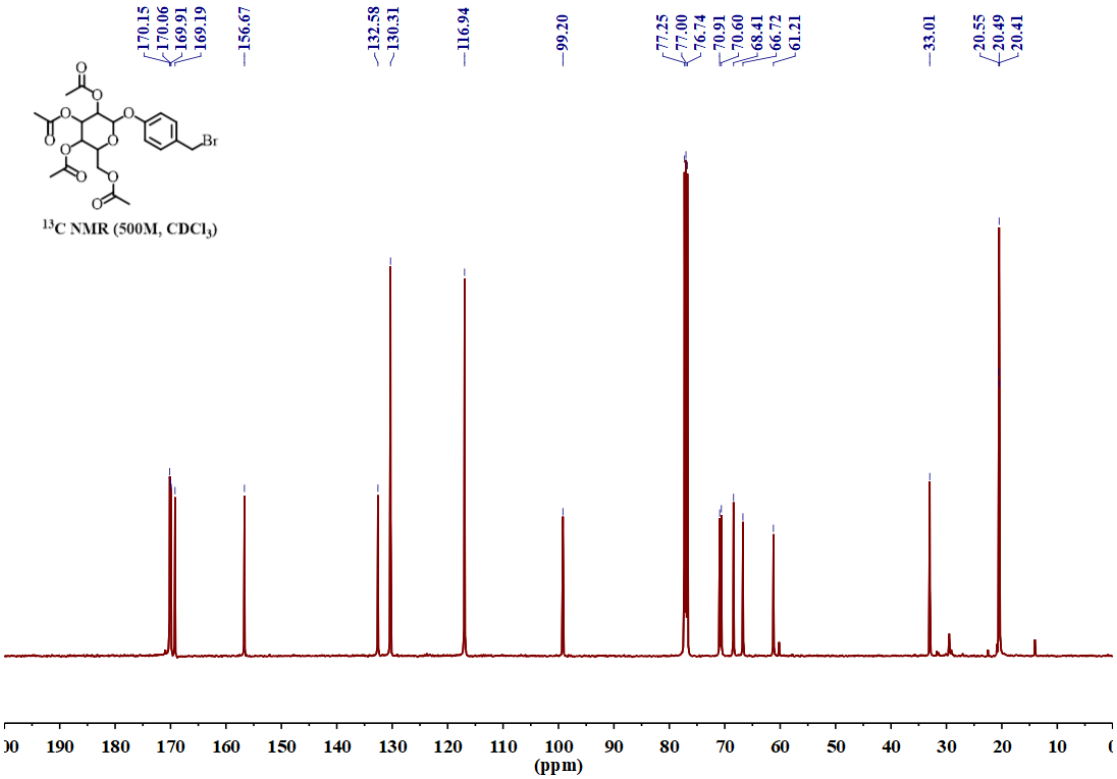

HRMS spectra of compound **c**

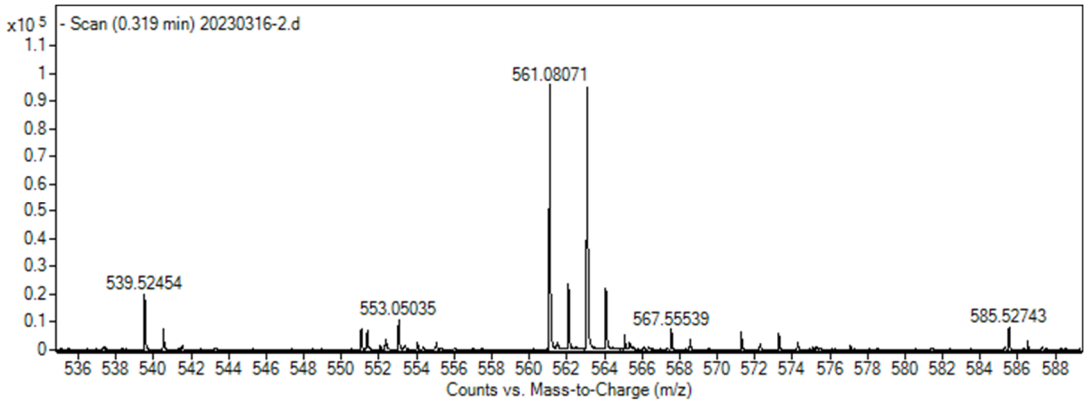

^{1}H NMR spectra of compound **d** in $CDCl_3$

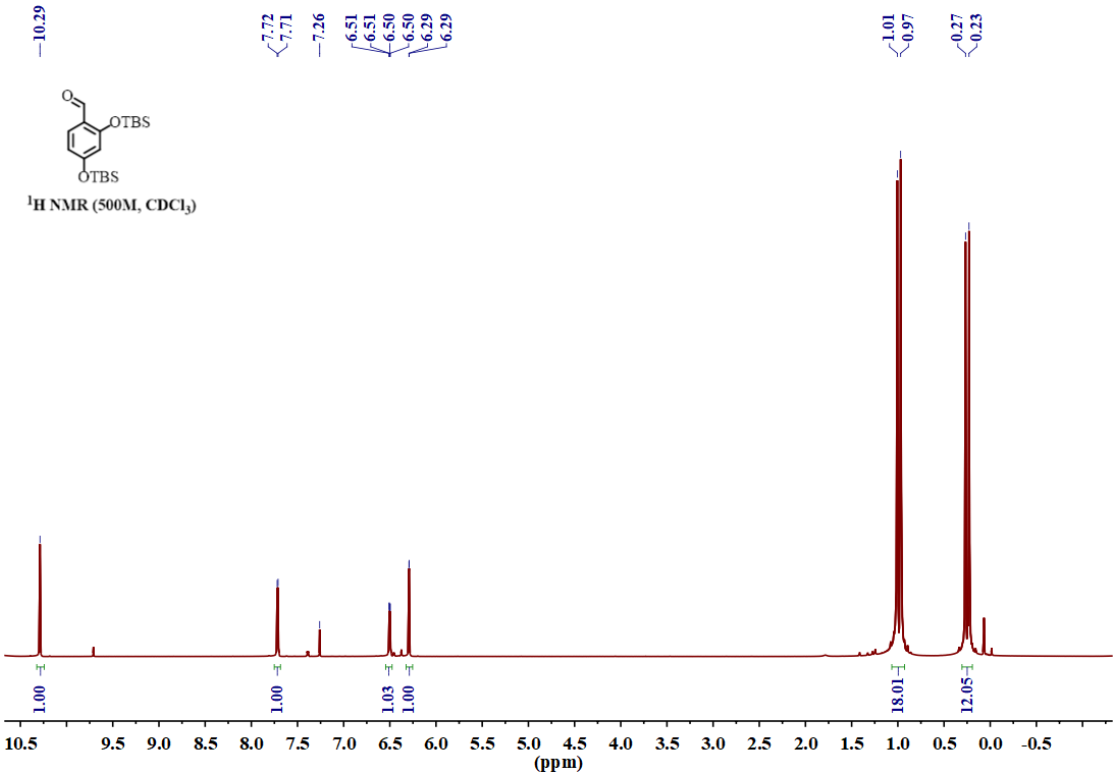

HRMS spectra of compound **d**

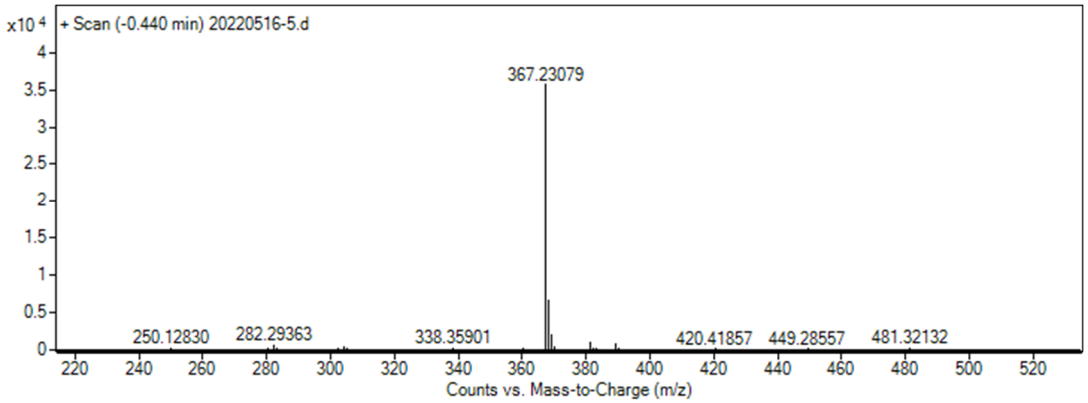

^{1}H NMR spectra of compound **e** in $CDCl_3$

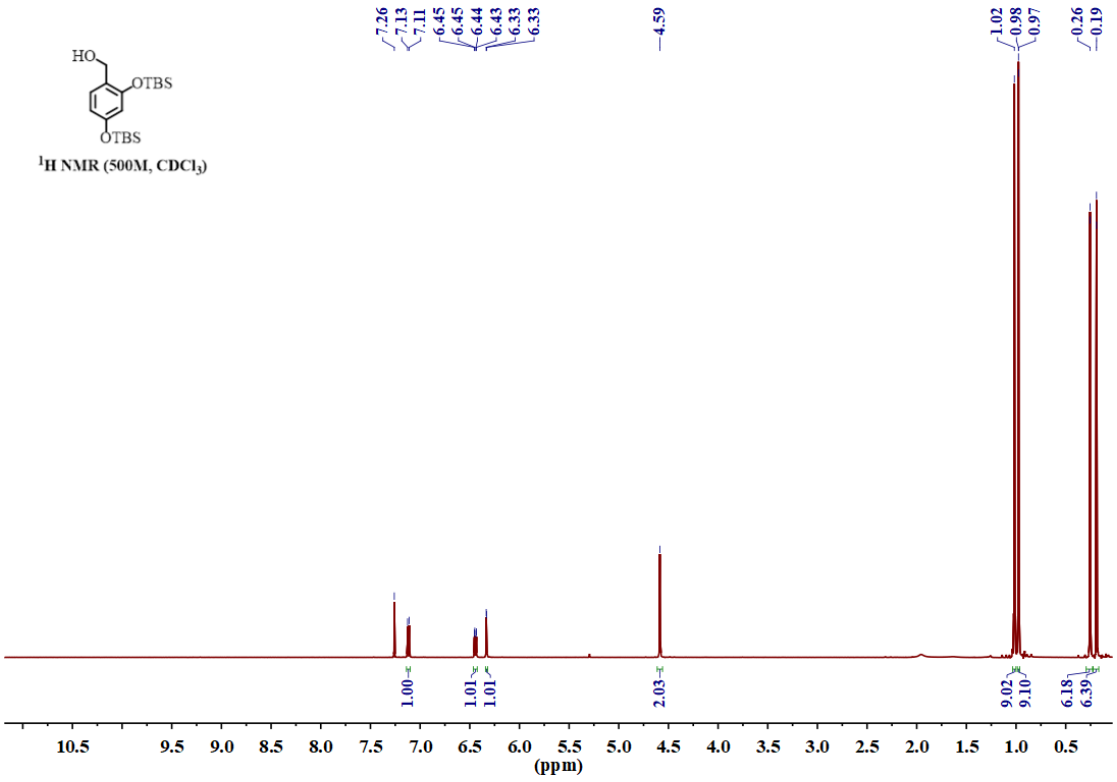

HRMS spectra of compound **e**

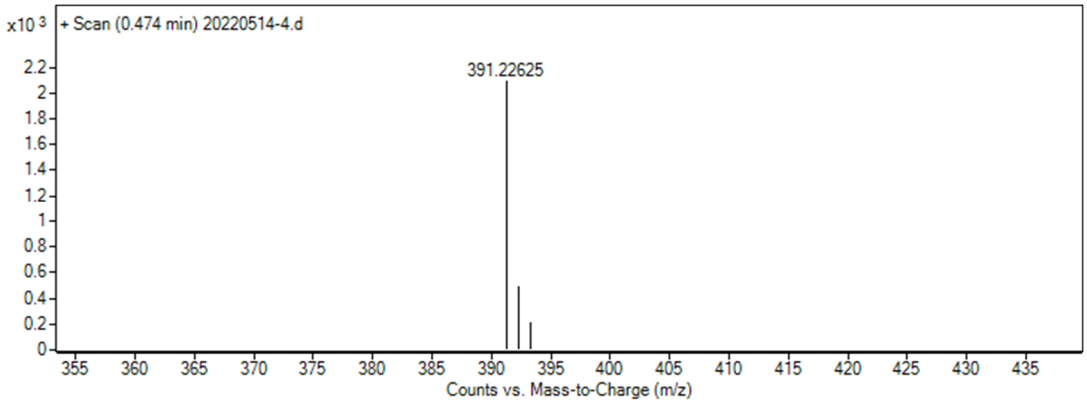

^{1}H NMR spectra of compound **f** in $CDCl_3$

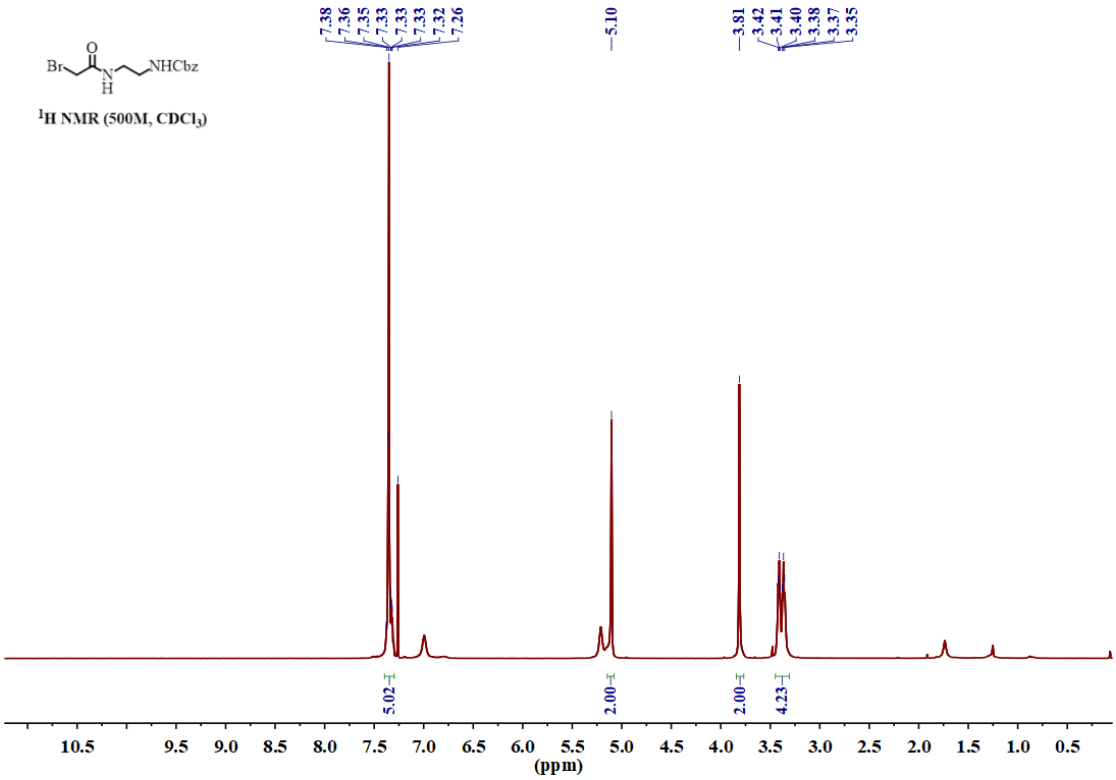

^{1}H NMR spectra of compound **1** in $CDCl_3$

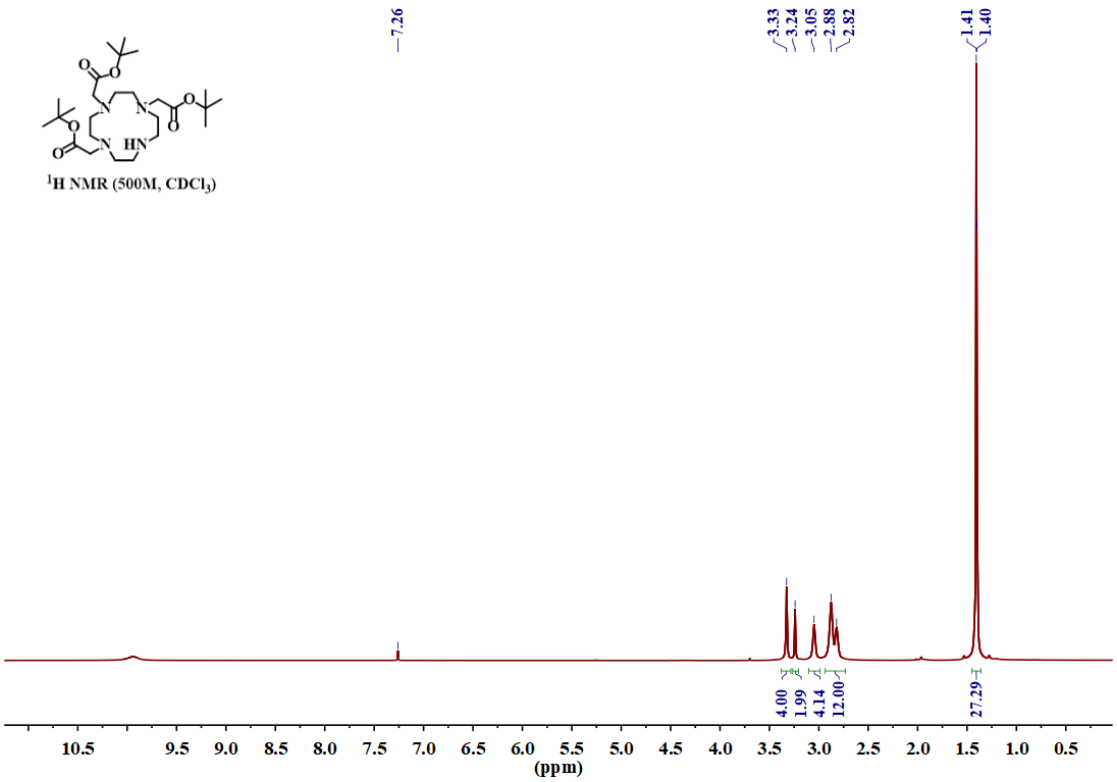

HRMS spectra of compound **1**

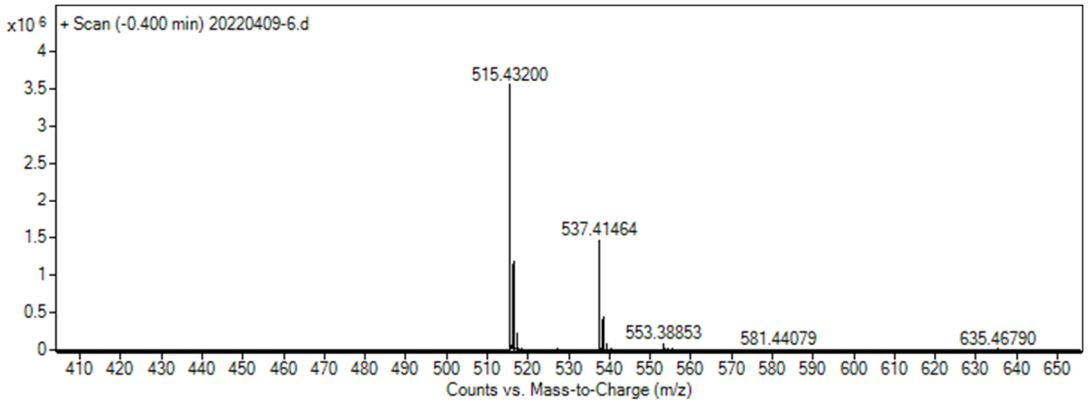

^{1}H NMR spectra of compound **2** in $CDCl_3$

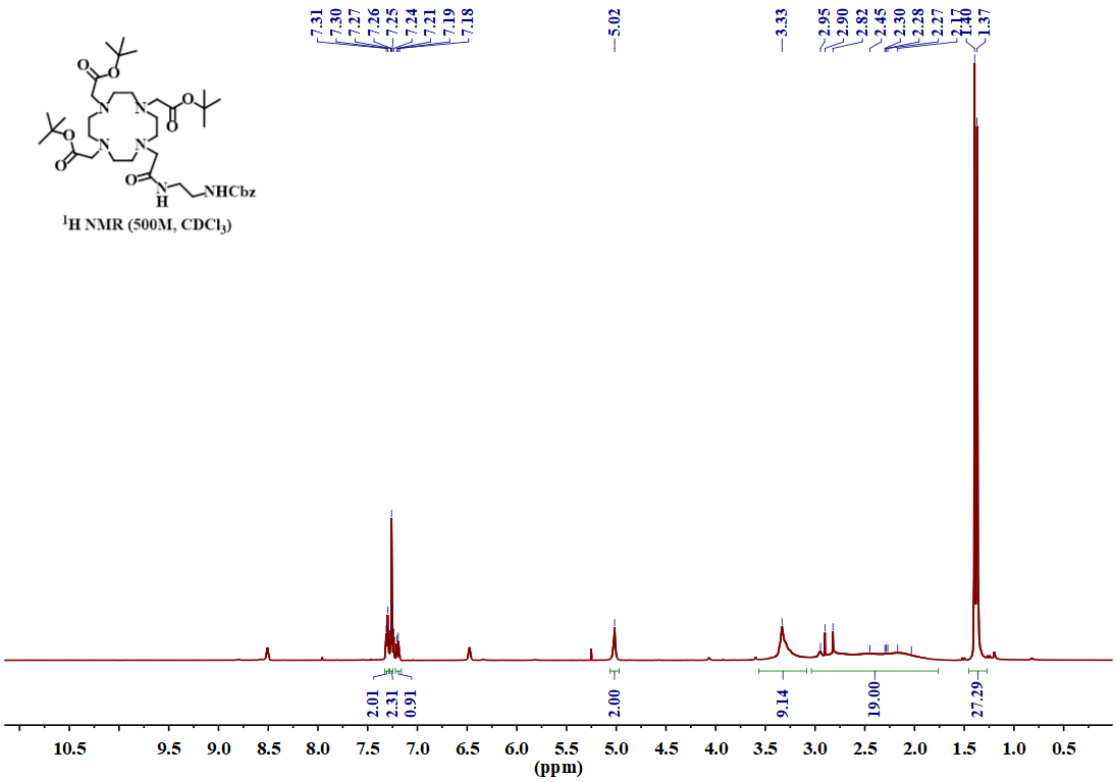

HRMS spectra of compound **2**

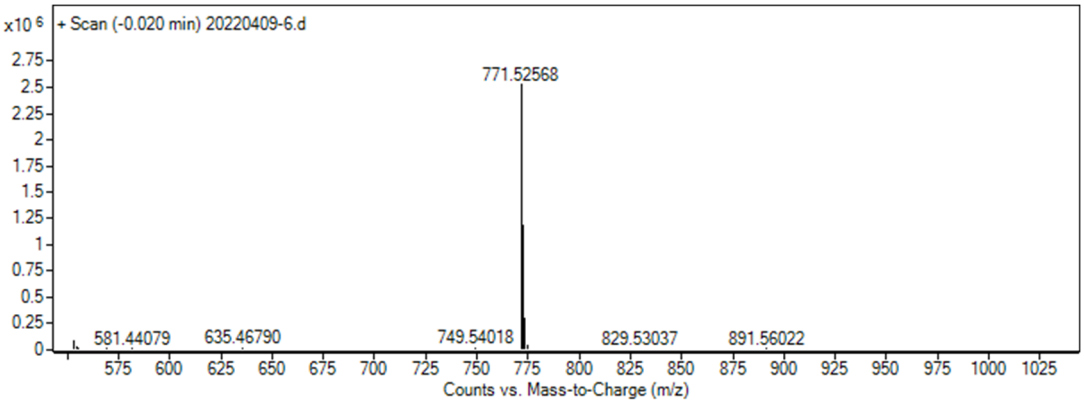

^{1}H NMR spectra of compound **3** in $CDCl_3$

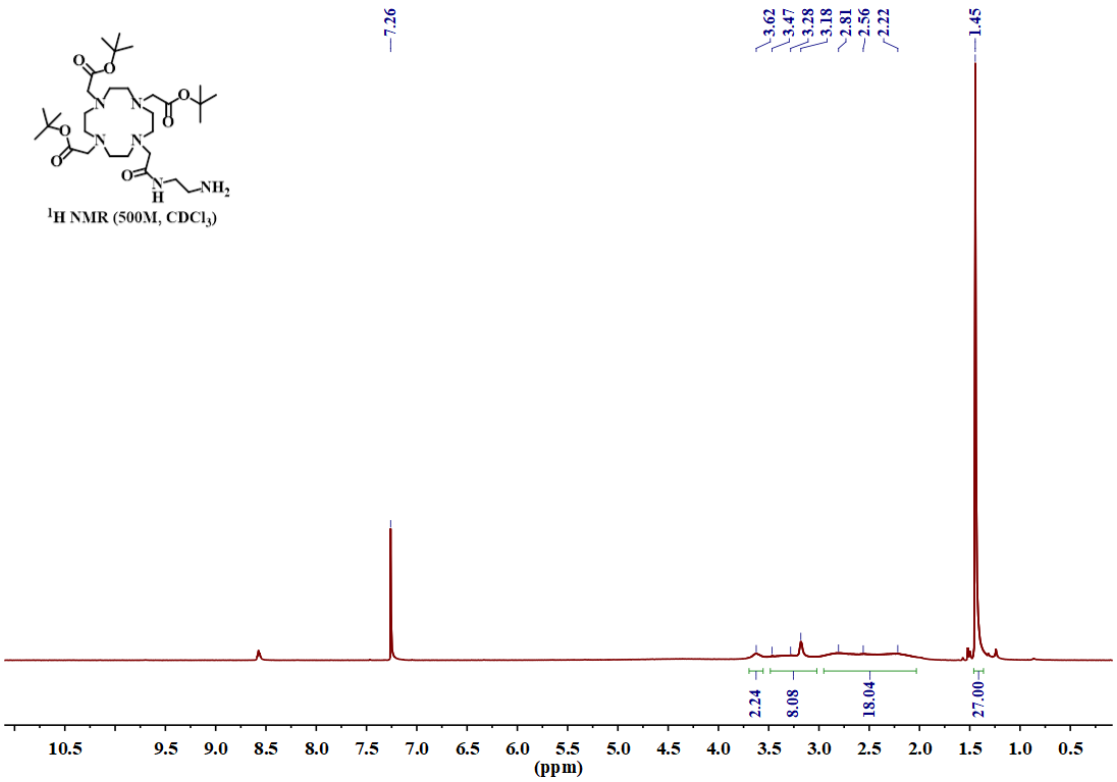

HRMS spectra of compound **3**

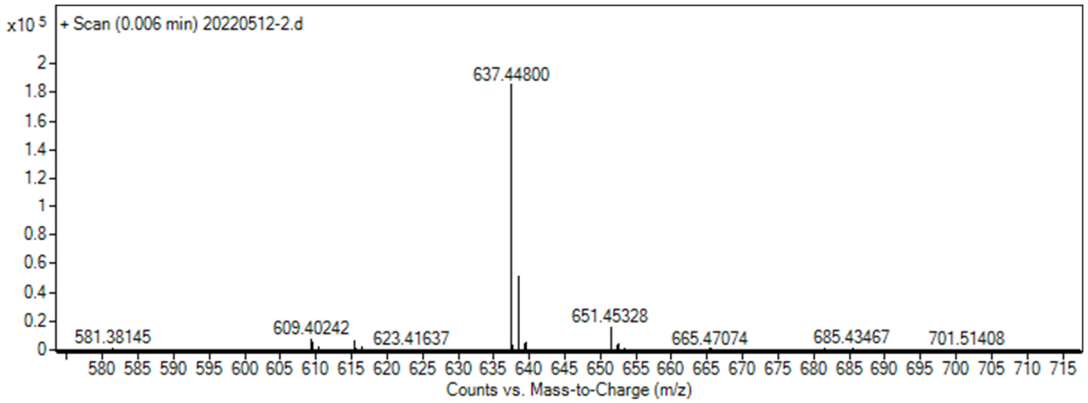

^{1}H NMR spectra of compound **4** in $CDCl_3$

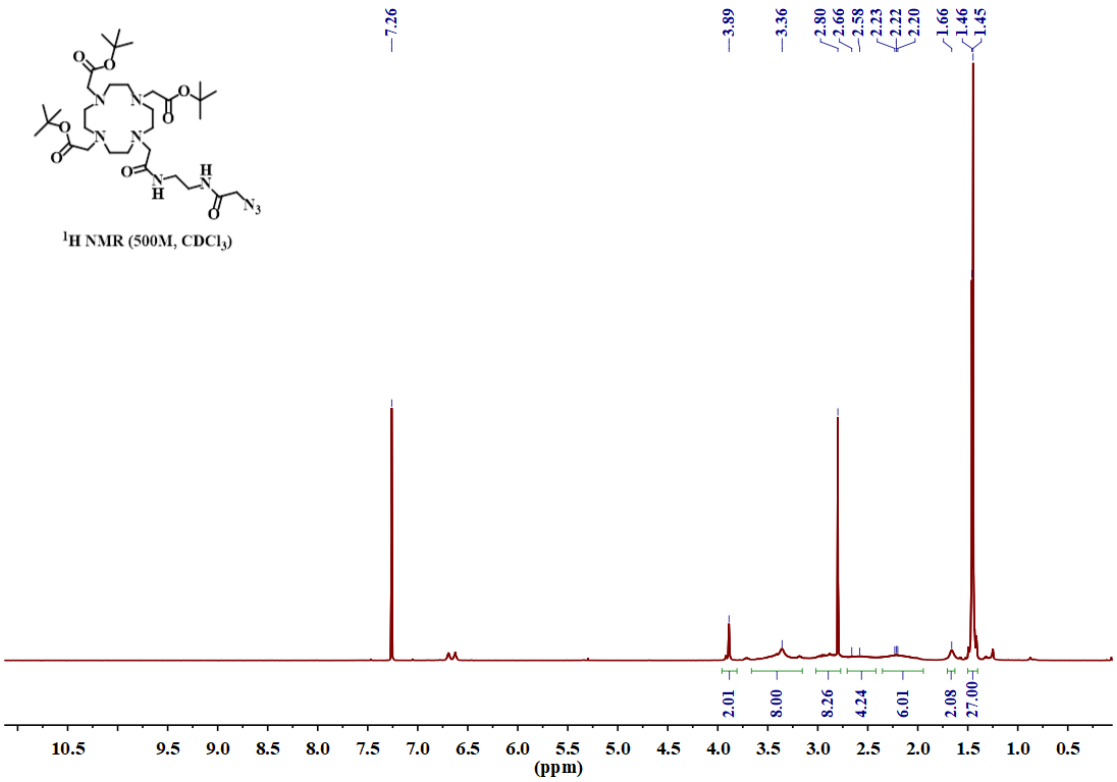

^{13}C NMR spectra of compound **4** in $CDCl_3$

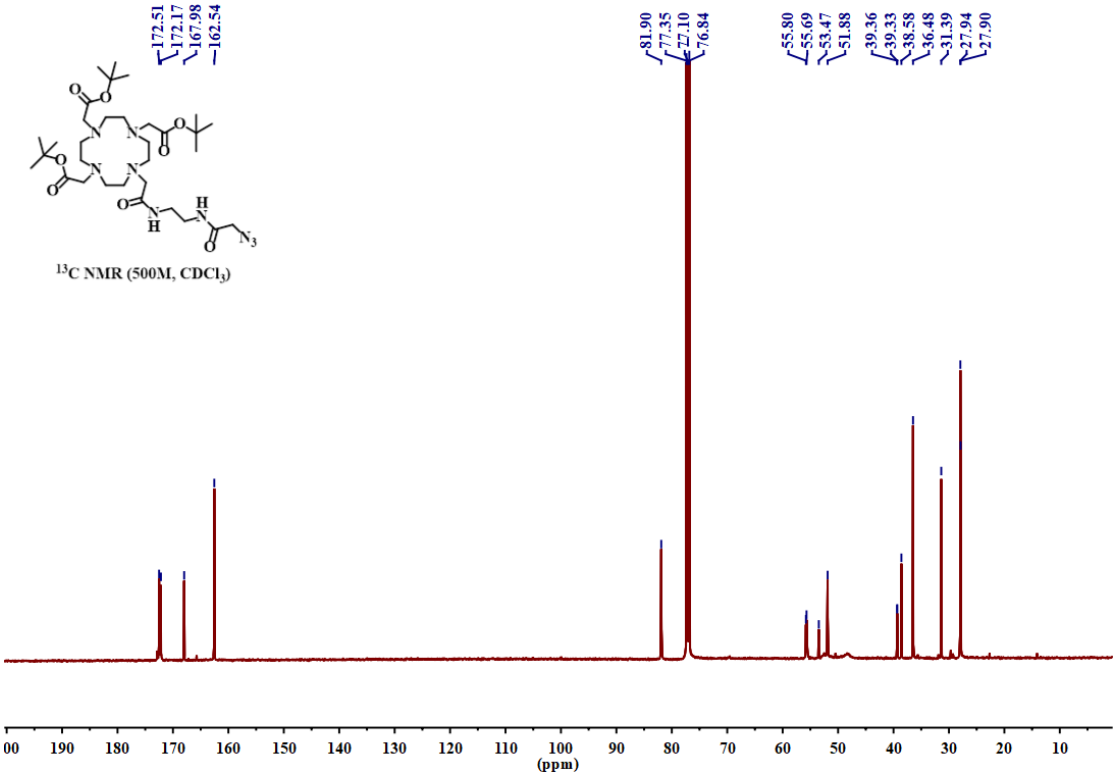

HRMS spectra of compound **4**

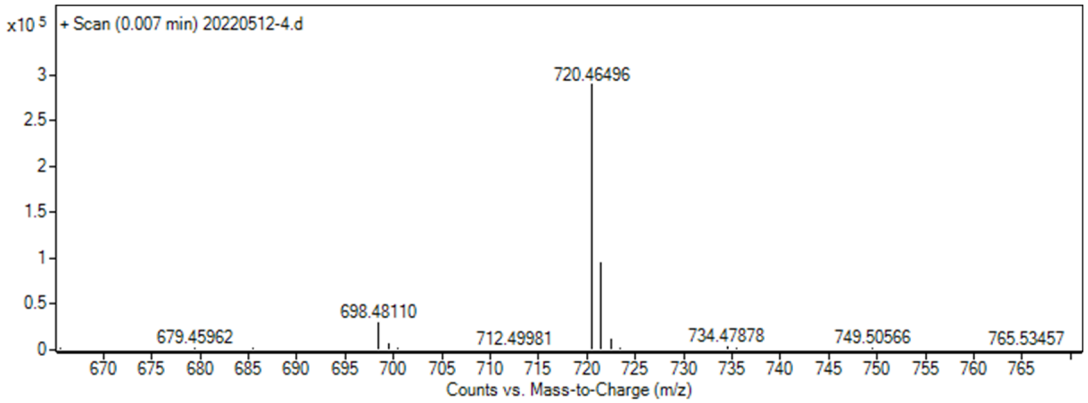

^{1}H NMR spectra of compound **7** in CD_3OD

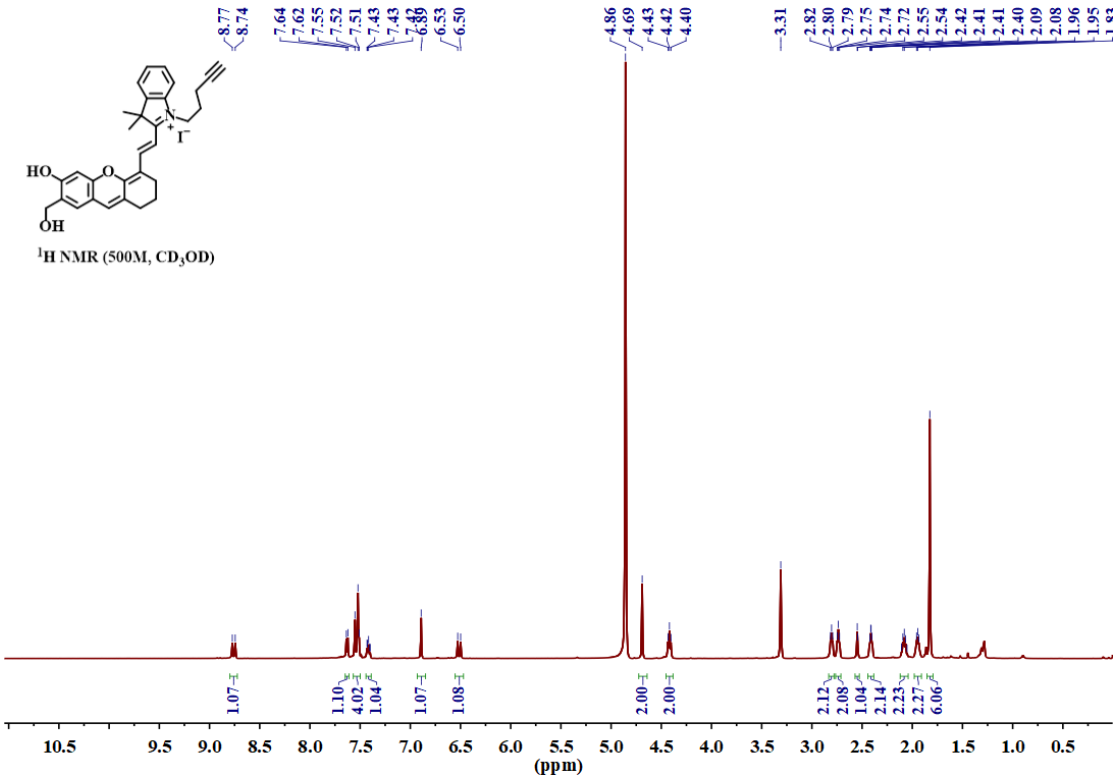

^{13}C NMR spectra of compound **7** in CD_3OD

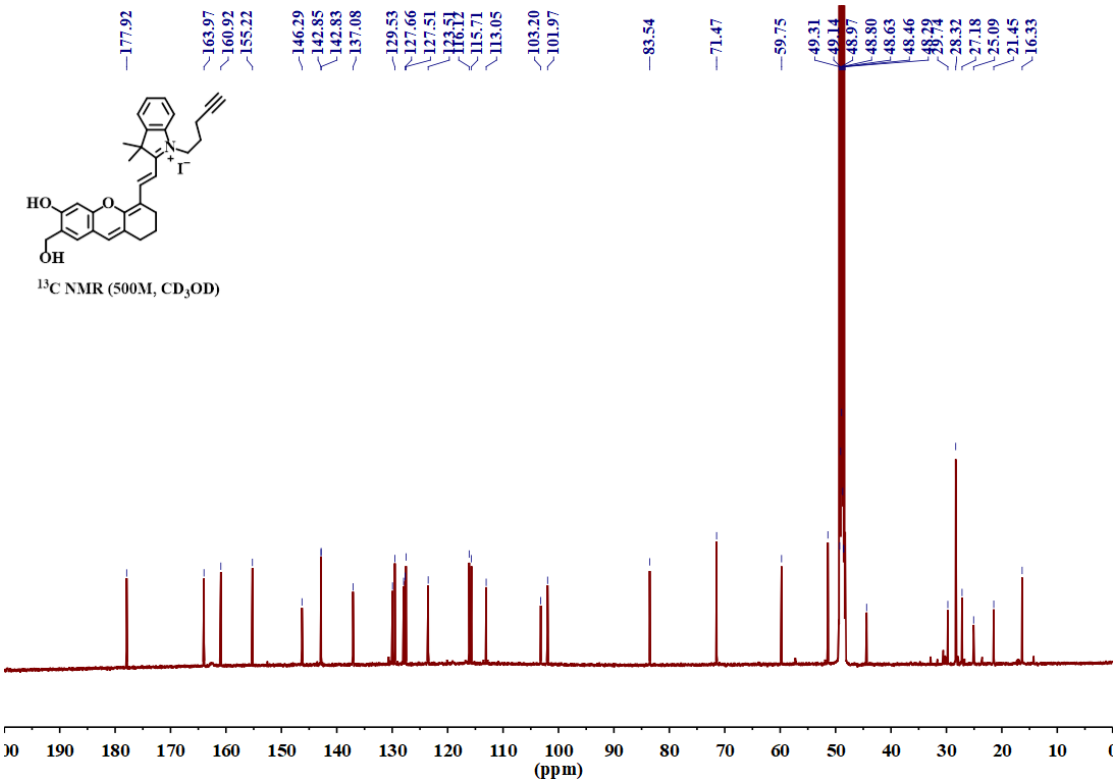

HRMS spectra of compound **7**

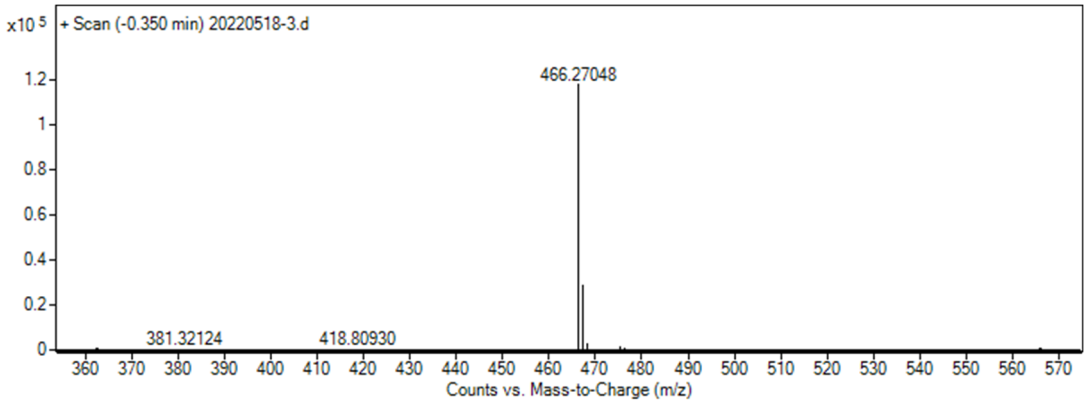

^{1}H NMR spectra of compound **8** in $CDCl_3$

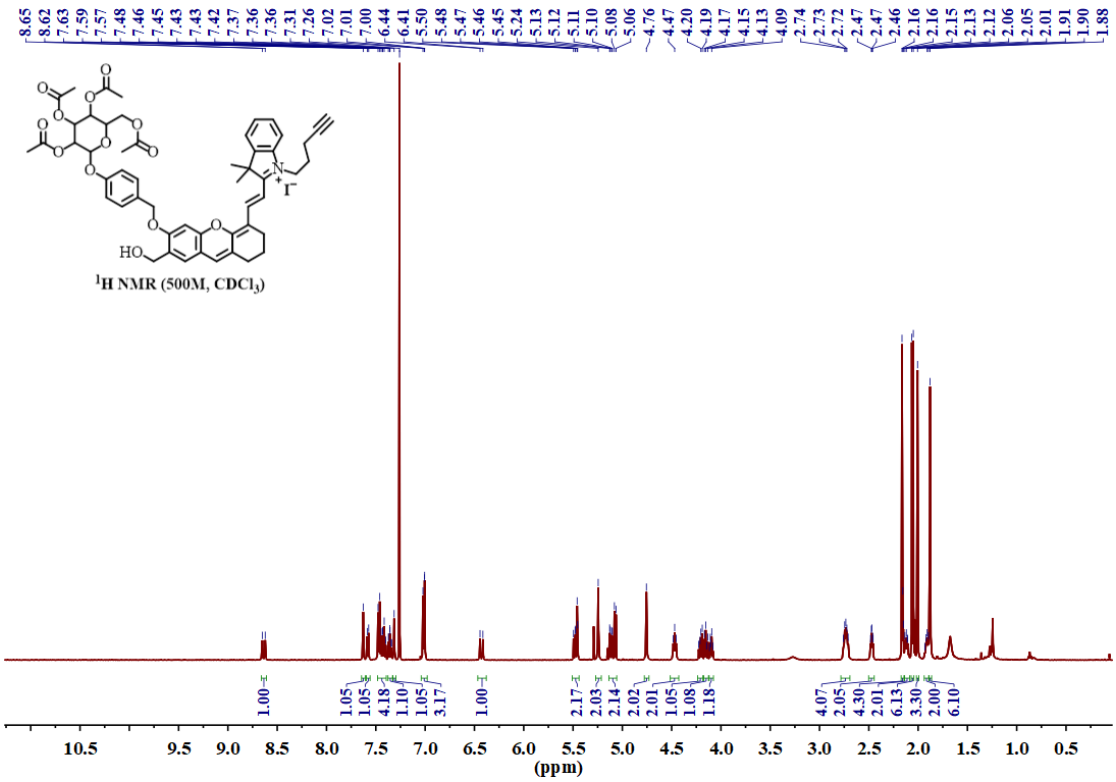

^{13}C NMR spectra of compound **8** in $CDCl_3$

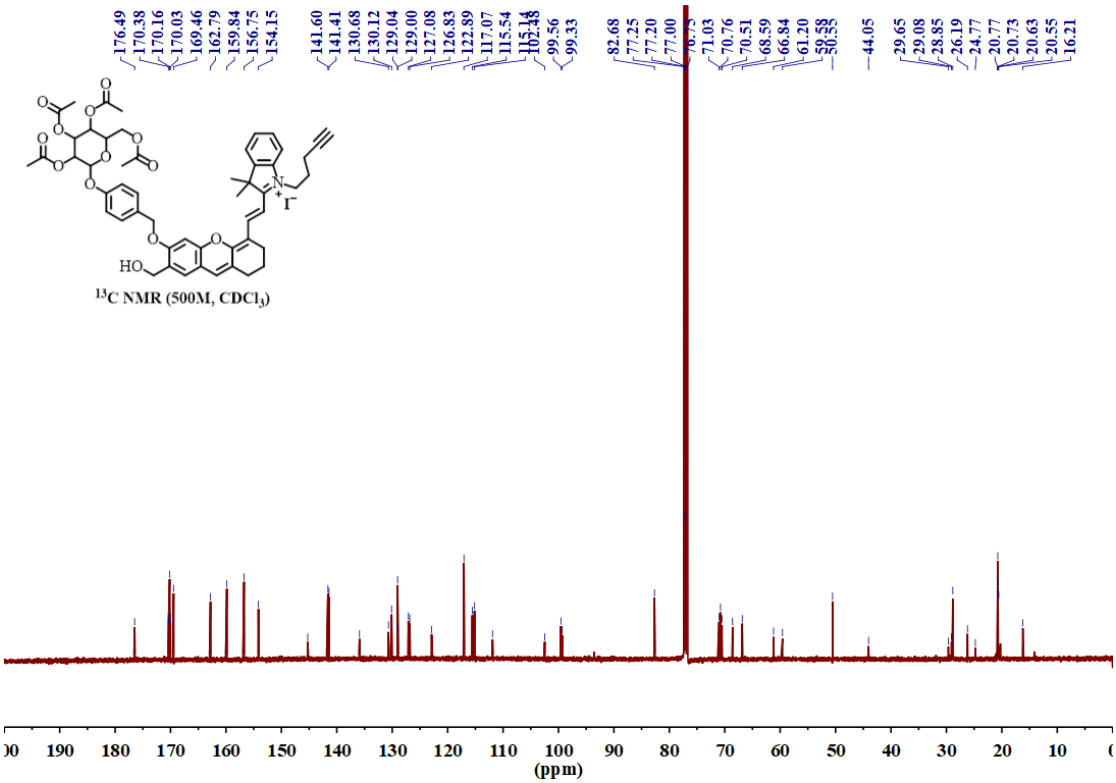

HRMS spectra of compound **8**

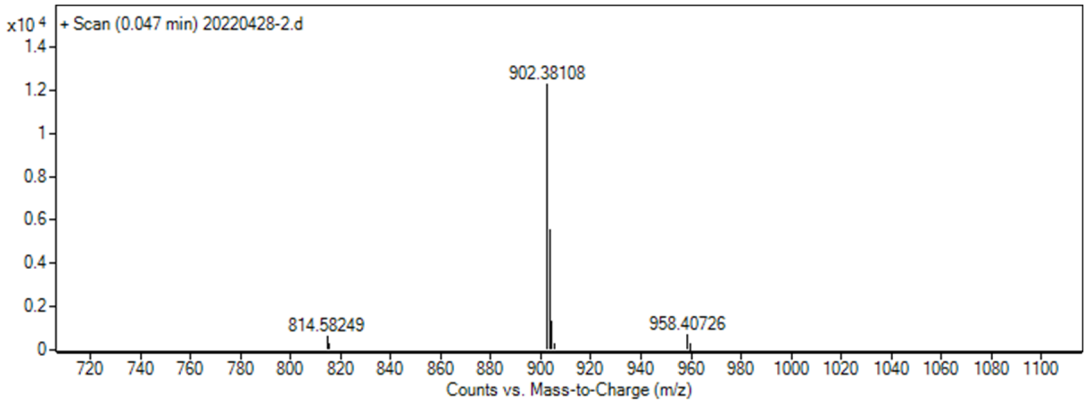

^{1}H NMR spectra of compound **9** in $CDCl_3$

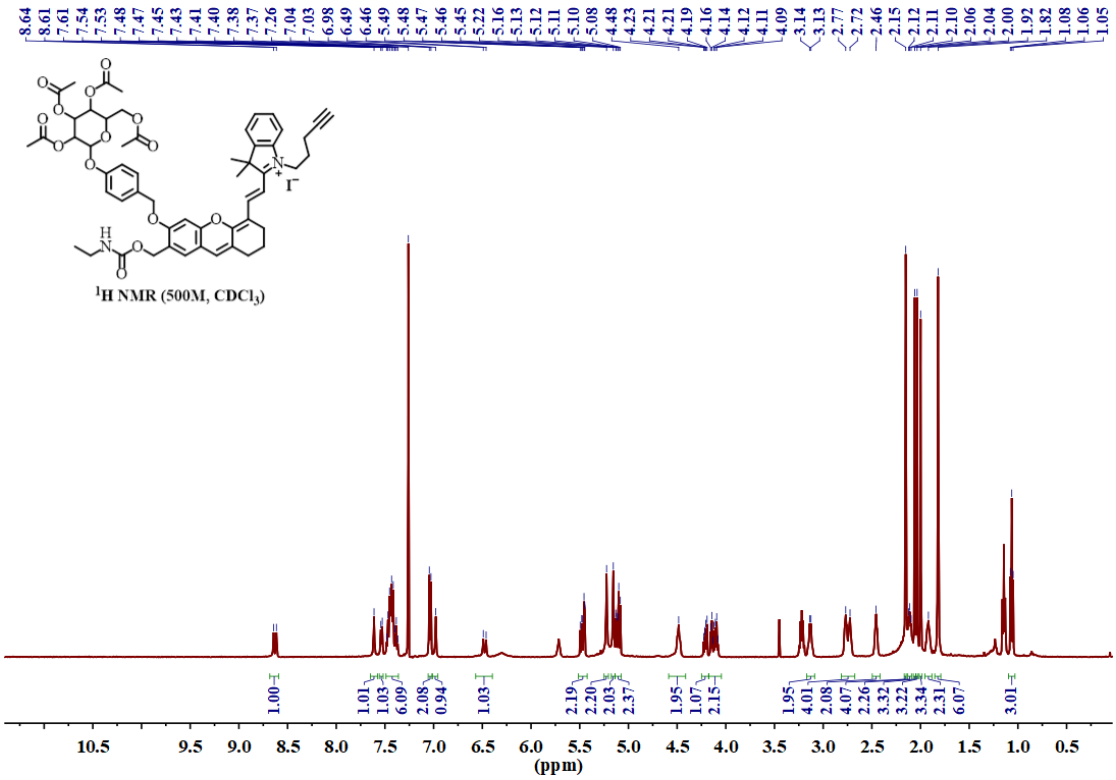

HRMS spectra of compound **9**

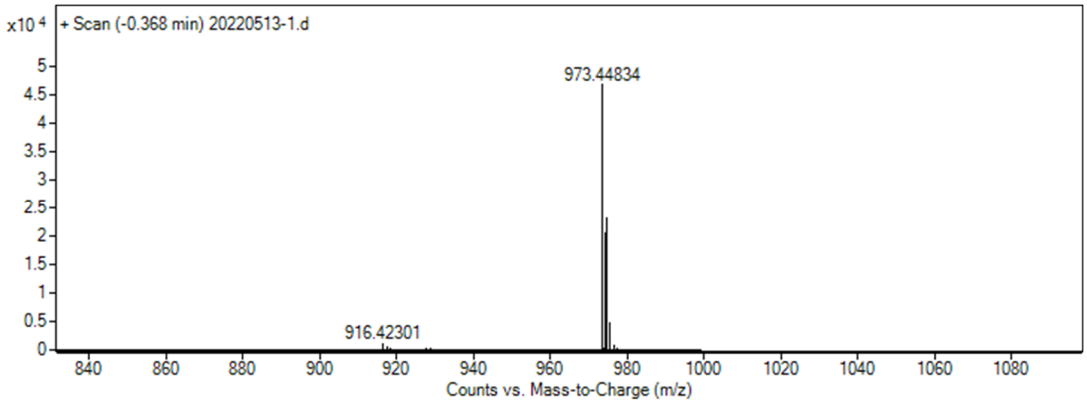

^{1}H NMR spectra of compound **10** in CD_3OD

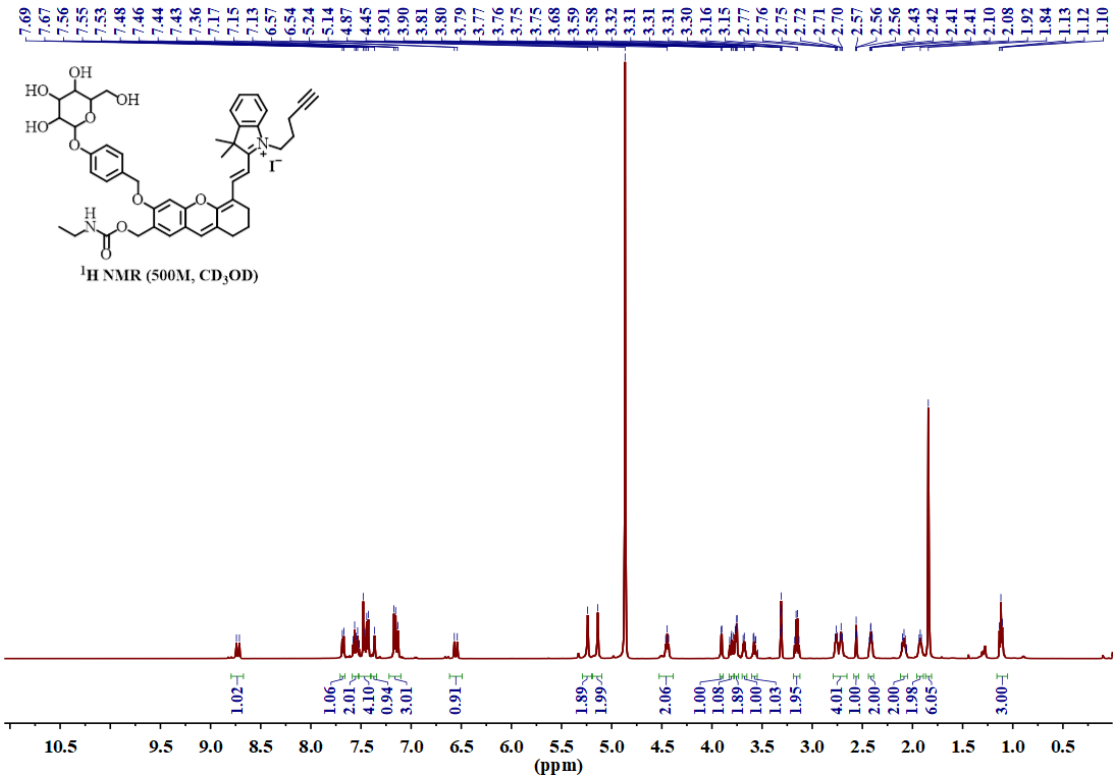

^{13}C NMR spectra of compound **10** in CD_3OD

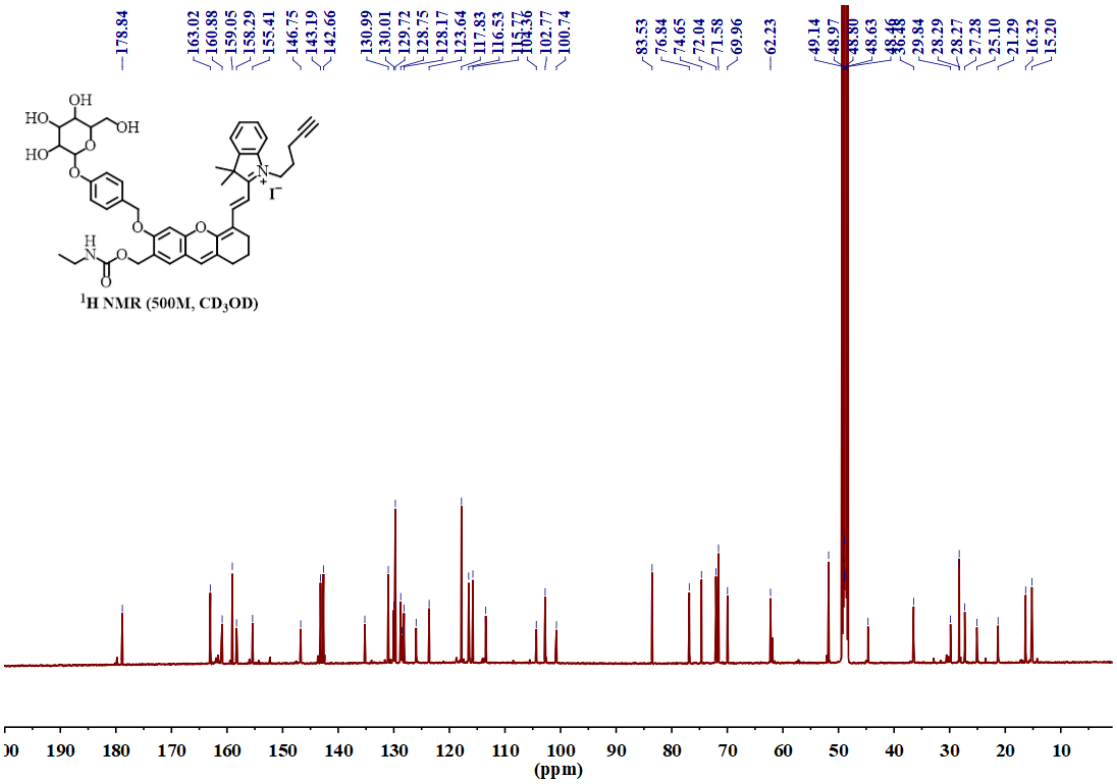

HRMS spectra of compound **10**

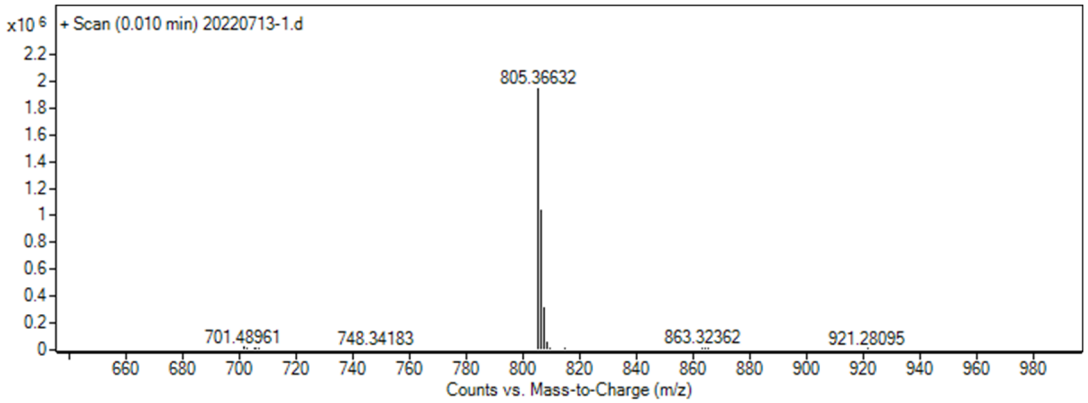

^{1}H NMR spectra of compound **12** in $CDCl_3$

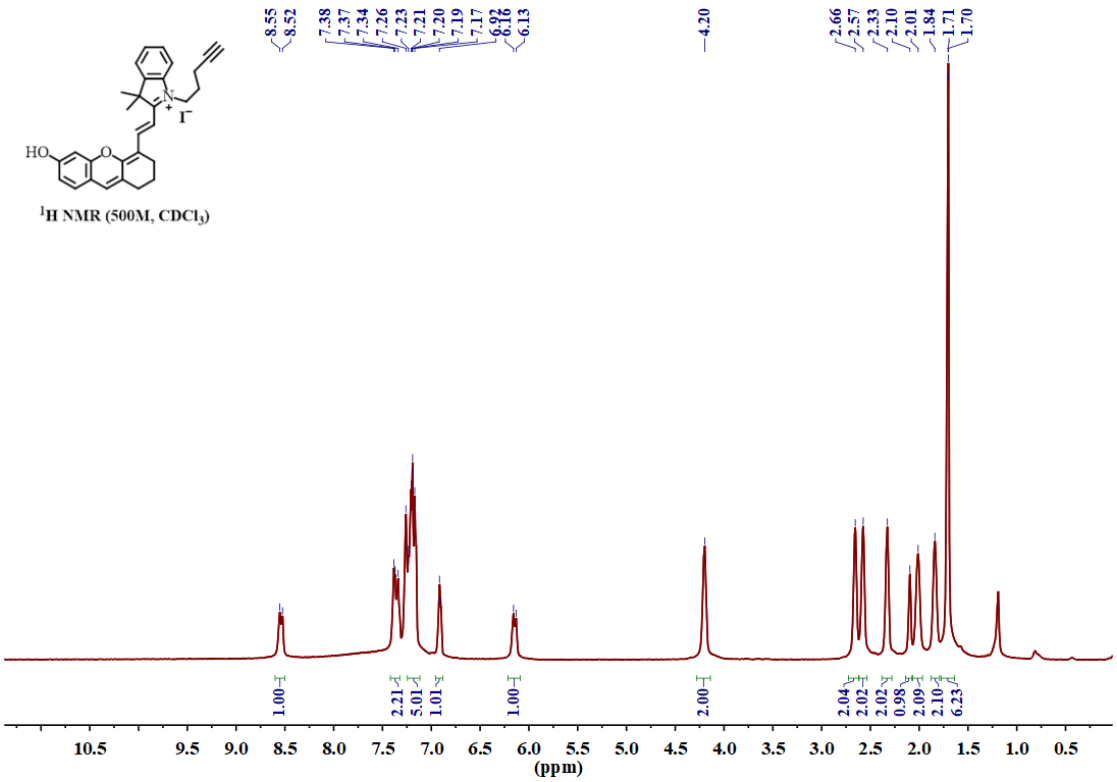

^{13}C NMR spectra of compound **12** in $CDCl_3$

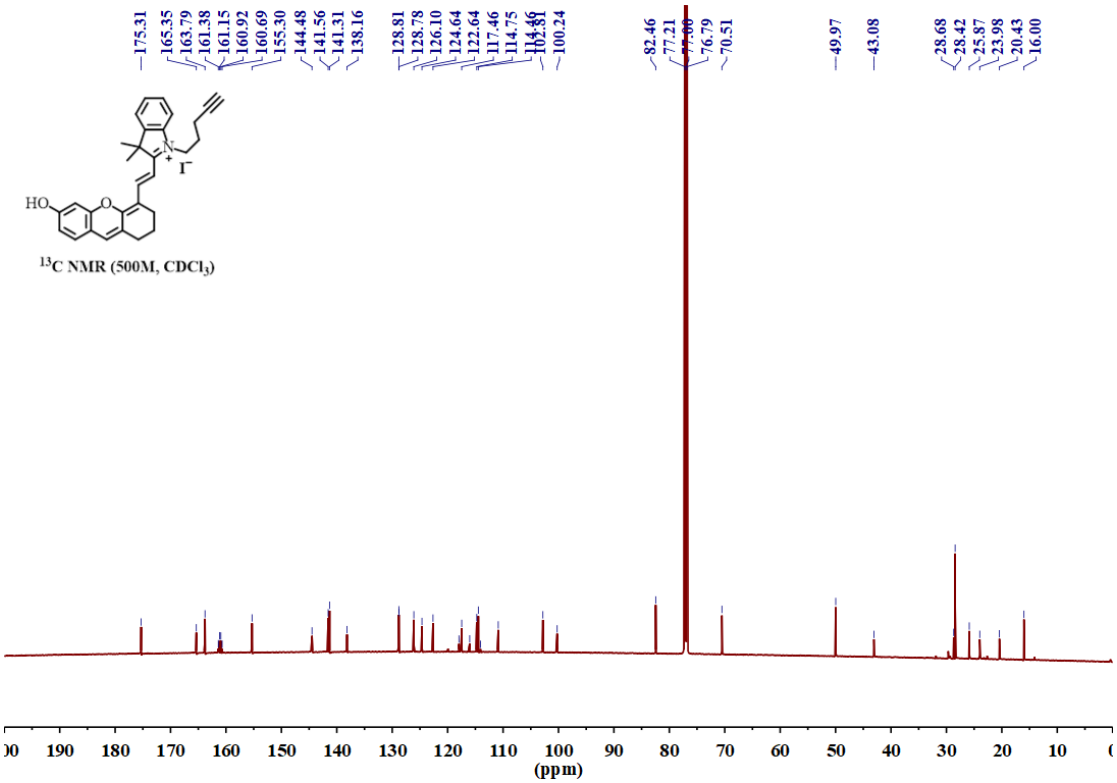

HRMS spectra of compound **12**

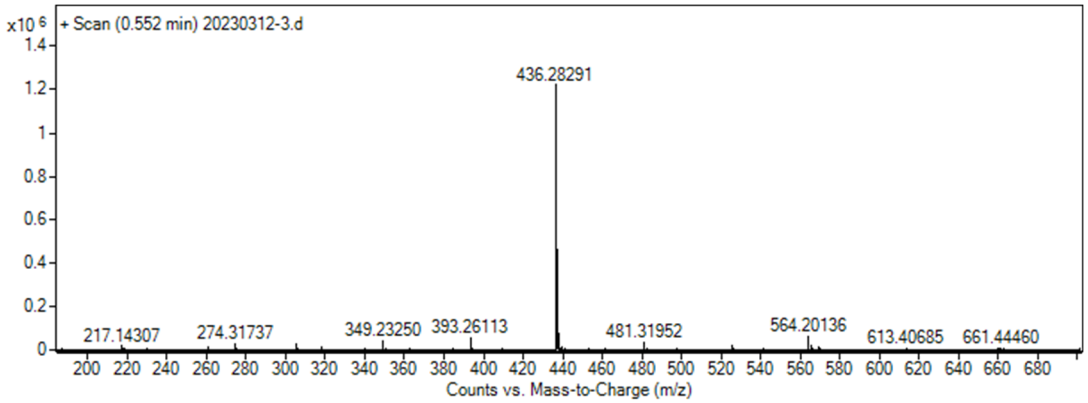

^{1}H NMR spectra of compound **13** in $CDCl_3$

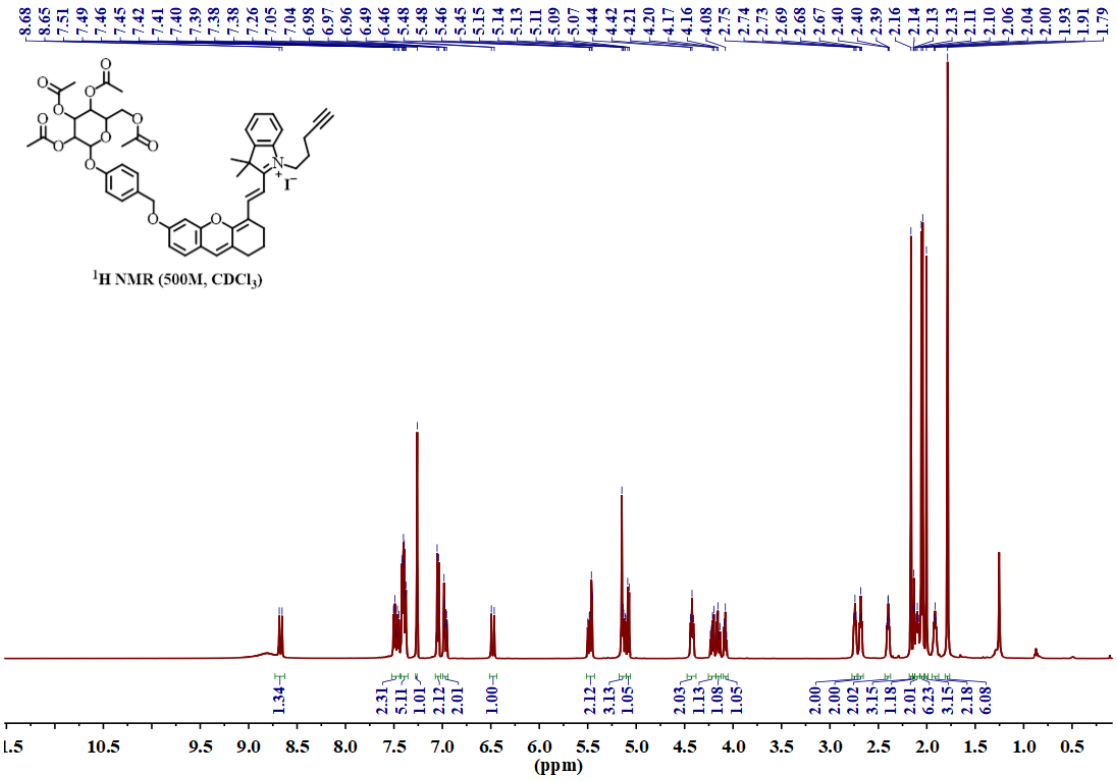

^{13}C NMR spectra of compound **13** in $CDCl_3$

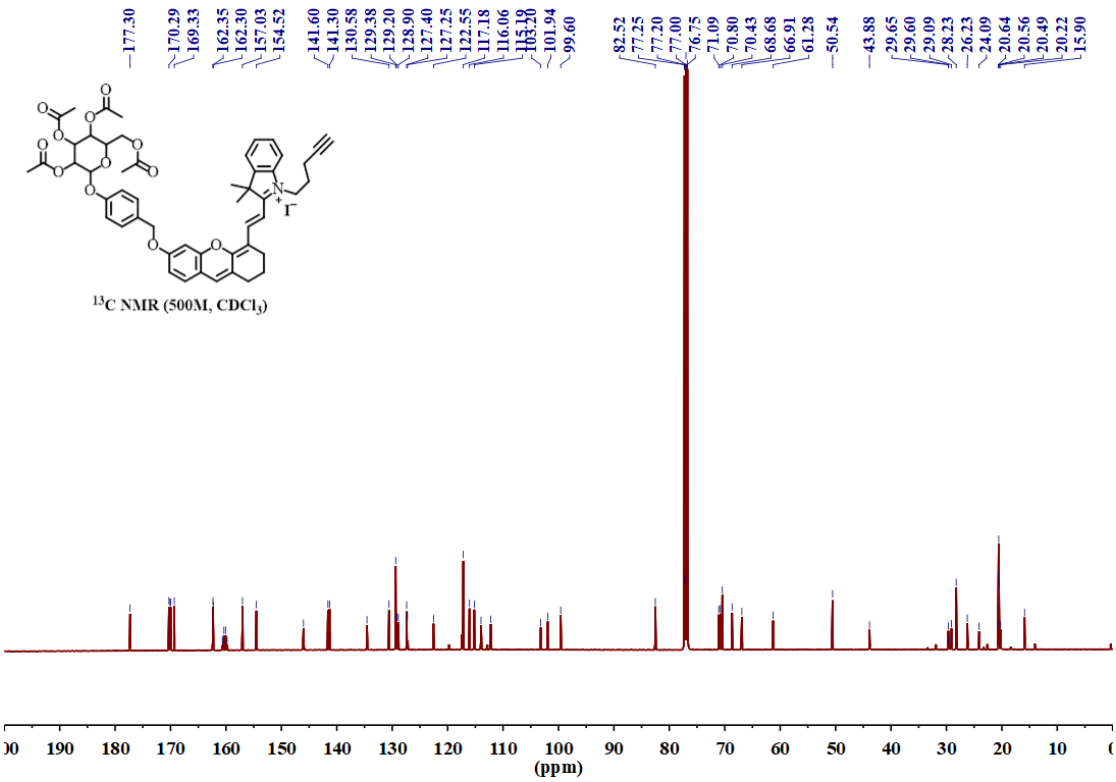

HRMS spectra of compound **13**

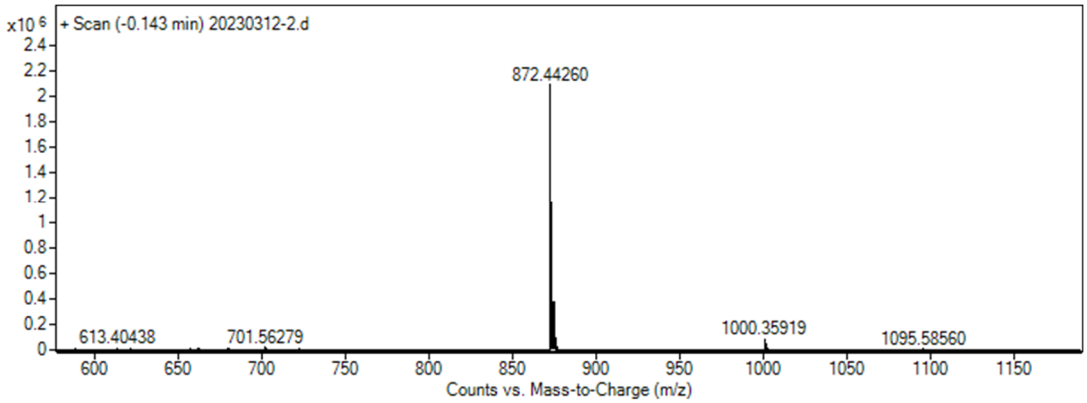

^{1}H NMR spectra of compound **14** in CD_3OD

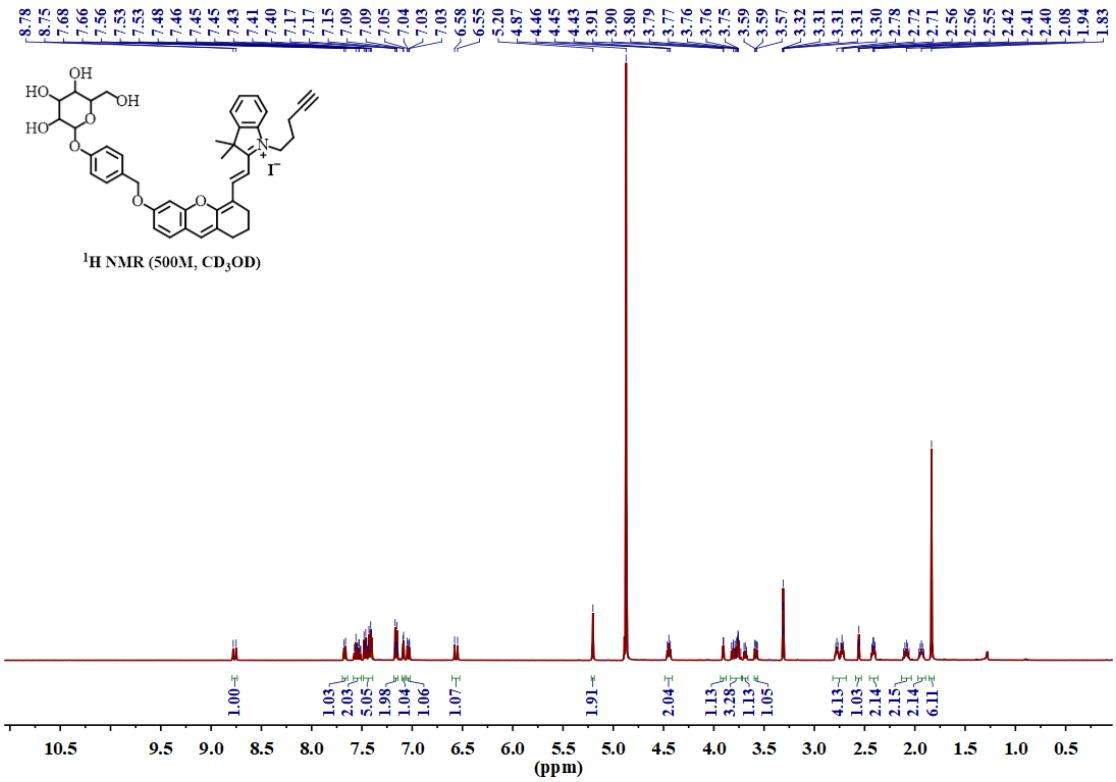

^{13}C NMR spectra of compound **14** in CD_3OD

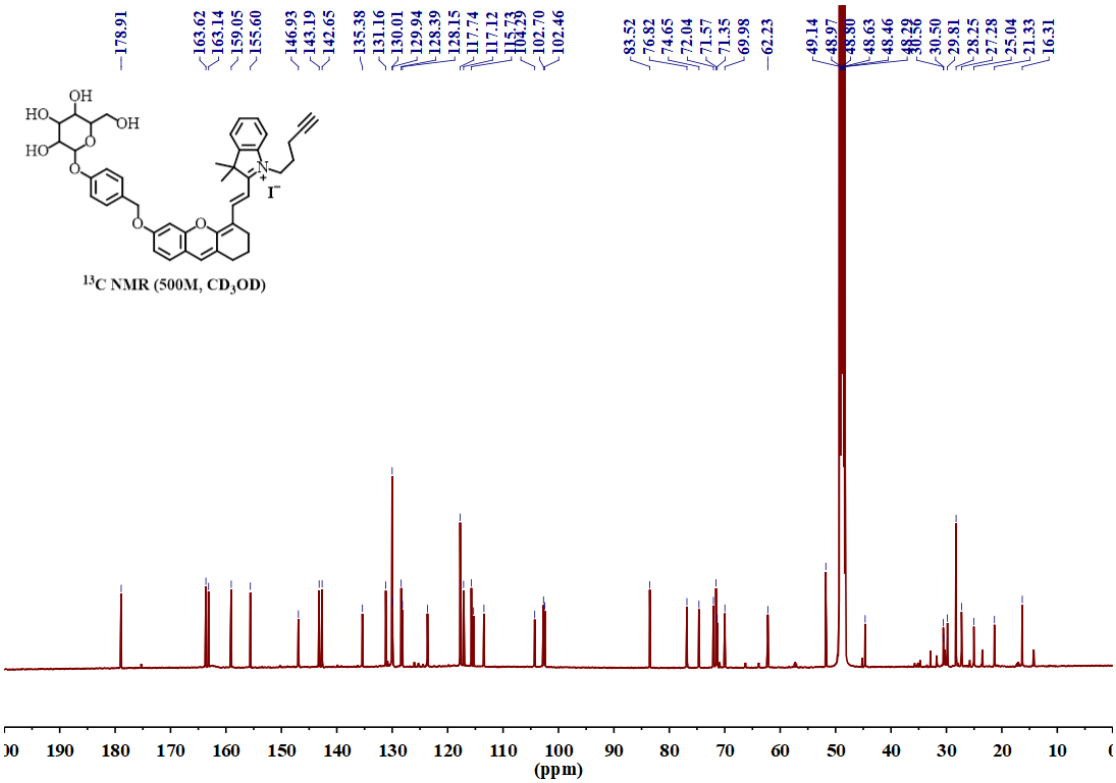

HRMS spectra of compound **14**